

Interactive comment on “Correction of real-time satellite precipitation with satellite soil moisture observations” by W. Zhan et al.

W. Wagner (Editor)

Both reviewers point out that it is not clear what this study adds to the paper published by Wanders et al. (2015) in Remote Sensing of Environment. This is a critical issue. Please make sure to address it in detail in your response.

Both referees address concerns regarding our novelties of our study compared to Wanders et al. (2015). We would like to highlight three aspects (line numbers are marked according to the updated manuscript attached):

(1) Wanders et al. (2015) tried to overcome the limitations in 3 hourly satellite precipitation retrievals by correcting them using satellite soil moisture and land surface temperature (LST) observations. One important conclusion by Wanders et al. (2015) is that their results showed the limited potential for using satellite soil moisture observations for correcting precipitation if “all-weather” – i.e. microwave based – land surface temperatures are available coincidentally and at a high spatial resolution as was the case with AMSR-E.

But this isn’t always the case, and it is also noted that current low-frequency microwave soil moisture missions (specifically SMAP and SMOS) don’t have radiometers at frequencies useful for estimating land surface temperatures. (We recognize that a 37 GHz sensor is part of the AMSR2 system, the frequency used from AMSR-E, but the equatorial crossing time for AMSR2 is 7.5 hours out of phase with SMAP and SMOS.) In fact these missions use LST from weather models analysis fields in their algorithms. Unfortunately the lowest microwave frequency of AMSR2 precludes retrieving soil moisture from many areas with heavy vegetation, and data availability of AMSR2 is significantly less than AMSR-E, which is no longer operable. Another advantage of SMAP and SMOS over AMSR2 is the increased penetration depth of the observations. This reduces the impact of the saturation problem and hence improves their potential for correcting precipitation estimates. So improvements to satellite precipitation from the Global Precipitation Mission products can be achieved using algorithms and satellite soil moisture products from SMAP and SMOS. This is an important motivation for the study and this goal has been clarified in the revision. (See *lines 82-121*). Thus, in our study, we focus exclusively on the usefulness of assimilating soil moisture products to improve satellite rainfall.

(2) We present in the paper improvements in the generation of rain particles and the bias-correction of the satellite soil moisture observations, as well as enhancements to the assimilation algorithm to maximize the information that can be gained from using soil moisture alone in adjusting precipitation. Due to the very strong and complicated spatial structure of precipitation, that is non-Gaussian and non-stationary in both time and space, a more advanced method is applied to generate possible precipitation fields than used or presented in earlier studies or in Wanders et al, (2015). Furthermore, a more advanced bias correction method is also applied to account for the reported problems (Wanders et al., 2015) in the second order statistics of the soil moisture retrievals (This has been clarified in *line 123-139*)

(3) Wanders et al. (2015) and previous studies are based on the assumption that the SM retrievals are 100% accurate and contain no errors. We evaluated this assumption by analyzing the impact of uncertainties associated with the soil moisture retrievals (added in *line 677-681*).

A new section has been added with detailed inter-comparisons with the current work. Please see Section 5 of the revised paper (*line 576-685*) for a more detailed description between our study and Wanders et al. (2015, *line 686-750*), including a quantitative comparison (*line 709-750*). Regarding comparisons to the earlier studies, we summarized previous finding and our novelties in *line 577-685*.

1 Correction of real-time satellite precipitation with 2 satellite soil moisture observations

3

4 Wang Zhan¹, Ming Pan¹, Niko ~~Wanders~~^{1,2}, Eric F. Wood¹

5 [1] Department of Civil and Environmental Engineering, Princeton University, Princeton,
6 NJ, USA

7 [2] Department of Physical Geography, Utrecht University, Utrecht, the Netherland

8

9 Abstract

10 Rainfall and soil moisture are two key elements in modeling the interactions between the
11 land surface and the atmosphere. Accurate and high-resolution real-time precipitation is
12 crucial for monitoring and predicting the on-set of floods, and allows for alert and
13 warning before the impact becomes a disaster. Assimilation of remote sensing data into a
14 flood-forecasting model has the potential to improve monitoring accuracy. Space-borne
15 microwave observations are especially interesting because of their sensitivity to surface
16 soil moisture and its change. In this study, we assimilate satellite soil moisture retrievals
17 using the Variable Infiltration Capacity (VIC) land surface model, and a dynamic
18 assimilation technique, a particle filter, to adjust the Tropical Rainfall Measuring Mission
19 Multi-satellite Precipitation Analysis (TMPA) real-time precipitation estimates. We
20 compare updated precipitation with real-time precipitation before and after adjustment
21 and with NLDAS gauge-radar observations. Results show that satellite soil moisture
22 retrievals provide additional information by correcting errors in rainfall bias. The
23 assimilation is most effective in the correction of medium rainfall under dry to normal
24 surface condition; while limited/negative improvement is seen over wet/saturated
25 surfaces. On the other hand, high frequency noises in satellite soil moisture impact the
26 assimilation by increasing rainfall frequency. The noise causes larger uncertainty in the

Authors 8/31/2015 3:38 PM

~~Deleted: Wanders²~~

Authors 8/31/2015 3:38 PM

~~Deleted: High accuracy soil moisture retrievals, when merged with precipitation, generally increase both rainfall frequency and intensity, and are~~

Authors 8/31/2015 3:38 PM

~~Deleted: Errors from soil moisture, mixed among~~

Authors 8/31/2015 3:38 PM

~~Deleted: real signal, may generate a~~

35 | false-alarmed rainfall over wet regions. A threshold of 2 mm/day soil moisture change is
36 | identified and applied to the assimilation, which masked out most of the noise.

Authors 8/31/2015 3:38 PM

Deleted: signal approximately 2mm

Authors 8/31/2015 3:38 PM

Deleted: and thus lower the precipitation accuracy after adjustment.

37
38

39 | 1 Introduction

40 | Precipitation is perhaps the most important variable in controlling energy and mass fluxes
41 | that dominate climate and particularly the terrestrial hydrological and ecological systems.
42 | Precipitation estimates, together with hydrologic models, provide the foundation for
43 | understanding the global energy and water cycles (Sorooshian, 2004; Ebert et al., 2007).
44 | However, obtaining accurate measurements of precipitation at regional to global scales
45 | has always been challenging due to its small-scale, space-time variability, and the sparse
46 | networks in many regions. Such limitations impede precise modeling of the hydrologic
47 | responses to precipitation. There is a clear need for improved, spatially distributed
48 | precipitation estimates to support hydrological modeling applications.

49 | In recent years, remotely sensed satellite precipitation has become a critical data source
50 | for a variety of hydrological applications, especially in poorly monitored regions such as
51 | sub-Saharan Africa due to its large spatial coverage. To date, a number of fine-scale,
52 | satellite-based precipitation estimates are now in operational production. One of the most
53 | frequently used is the Tropical Rainfall Measuring Mission Multi-satellite Precipitation
54 | Analysis (TMPA) product (Huffman et al., 2007). Over the 17 years lifetime since the
55 | launch of the Tropical Rainfall Measuring Mission (TRMM) in 1997, a series of high
56 | resolution (0.25-degree and 3-hourly), quasi-global (50°S - 50°N), near-realtime,
57 | TRMM-based precipitation estimates have been developed and made available to the
58 | research and applications communities (Huffman et al., 2007; 2010). Flood forecasting
59 | and monitoring is one major application for real time satellite rainfall products (Wu et al,
60 | 2014). However, the applicability of satellite precipitation products for near real-time
61 | hydrological applications that include drought and flood monitoring has been hampered
62 | by their need for gauge-based adjustment.

66 While it is possible to create such estimates solely from one type of sensor, researchers
67 have increasingly moved to using combinations of sensors in an attempt to improve
68 accuracy, coverage and resolution. A promising avenue for rainfall correction is through
69 the assimilation of satellite-based surface soil moisture into a water balance model (Pan
70 and Wood, 2006). Over land, the physical relationship between variations in soil water
71 storage and rainfall accumulation contain complementary information that can be
72 exploited for the mutual benefit of both types of products (Massari et al., 2014; Crow et
73 al., 2009). Unlike instantaneous rain rate, satellite surface soil moisture retrievals utilize
74 low frequency microwave signals and possess some memory reflecting antecedent
75 rainfall amounts.

76 Studies have demonstrated that in situ (Brocca et al., 2009, 2013; Matgen et al., 2012)
77 and satellite (Francois et al., 2003; Pellarin et al., 2008, 2013; Brocca et al., 2014)
78 estimates of surface soil moisture could contribute to precipitation estimates by providing
79 useful information concerning the sign and magnitude of antecedent rainfall
80 accumulation errors. In particular, Brocca et al. (2014) estimated daily rainfall on a global
81 scale based on satellite SM products by inverting the soil water balance equation. Crow et
82 al. (2003, 2009, 2011) corrected space-borne rainfall retrievals by assimilating remotely
83 sensed surface soil moisture retrievals into an Antecedent Precipitation Index (API) based
84 soil water balance model using a Kalman filter (Kalman, 1960). However, these studies
85 focused on multi-day aggregation periods and a space aggregated correction at 1°
86 resolution for the corrected precipitation totals. This limits their applicability in
87 applications such as near real-time flood forecasting. Wanders et al. (2015) tried to
88 overcome this limitation by the correction of 3 hourly satellite precipitation totals with a
89 set of satellite soil moisture and land surface temperature observations. One important
90 conclusion by Wanders et al. (2015) is that their results showed the limited potential for
91 satellite soil moisture observations for correcting precipitation if “all-weather” – i.e.
92 microwave based – land surface temperatures are available coincidently and at high
93 spatial resolution as was the case with AMSR-E.

94 But this isn't always the case, and it is also noted that current low-frequency microwave
95 soil moisture missions (specifically SMAP and SMOS) don't have radiometers at

Authors 8/31/2015 3:38 PM

Deleted: spaceborne

Authors 8/31/2015 3:38 PM

Deleted: a simple

Authors 8/31/2015 3:38 PM

Deleted: The hydrologic response

Authors 8/31/2015 3:38 PM

Deleted: to precipitation is especially

Authors 8/31/2015 3:38 PM

Deleted: in

Authors 8/31/2015 3:38 PM

Deleted: an explicit and sophisticated physical model is needed to accurately recover

Authors 8/31/2015 3:38 PM

Deleted: information about the rainfall more precisely, e.g. wetted area. This is because most storm systems have a very strong and complicated spatial structure that is non-Gaussian and non-stationary in both time and space (Wanders et al., 2015).

Authors 8/31/2015 3:38 PM

Deleted: In this paper we present a method to improve real-time remote sensing precipitation products by merging retrievals with soil moisture remote sensing products through a Particle Filter (PF),

114 [frequencies useful for estimating land surface temperatures, even though a 37 GHz sensor](#)
115 [is part of the AMSR2 system. In fact SMAP and ECMWF/SMOS use LST from weather](#)
116 [models analysis fields in their algorithms. Unfortunately the lowest microwave](#)
117 [frequency of AMSR2 precludes retrieving soil moisture from many areas with heavy](#)
118 [vegetation, and data availability of AMSR2 is significantly less than AMSR-E, but is no](#)
119 [longer operable. So improvements to satellite precipitation from the Global Precipitation](#)
120 [Mission products must rely solely on satellite soil moisture products from SMAP and](#)
121 [SMOS, and the improvements to the assimilation algorithms is the goal of this study.](#)

122 [Thus, we focus exclusively on the usefulness of assimilating soil moisture products to](#)
123 [improve satellite rainfall. We propose as part of the work how to improve the generation](#)
124 [of rain particles and the bias-correction of the satellite soil moisture observations, as well](#)
125 [as to enhance the assimilation algorithm to maximize the information that can be gained](#)
126 [from using soil moisture alone to adjust precipitation. Due to the very strong and](#)
127 [complicated spatial structure of precipitation, that is non-Gaussian and non-stationary in](#)
128 [both time and space \(Wanders et al., 2015\), a more advanced method is applied to](#)
129 [generate possible precipitation fields than were used in earlier studies or in Wanders et al.](#)
130 [2015\) \(see section 2.2.2\). Furthermore, a more advanced bias correction method is also](#)
131 [applied to account for the reported problems in the second order statistics of the soil](#)
132 [moisture retrievals. We used a soil moisture remote sensing product to improve real-time](#)
133 [remote sensing precipitation product, TMPA 3B42RT, through a Particle Filter \(PF\) and](#)
134 [therefore offer an improved basis for quantitatively monitoring and predicting flood](#)
135 [events, especially in those parts of the world where in-situ networks are too sparse to](#)
136 [support more traditional methods of hydrologic monitoring and prediction. The](#)
137 [precipitation enhancement experiments are carried out over the continental U.S.](#)
138 [\(CONUS\) and the precipitation skill is validated against the NLDAS gauge-radar](#)
139 [precipitation product. Section 5 presents a comparison of the results from this study to](#)
140 [the earlier studies related to improving satellite precipitation.](#)

141 **2 Methods**

142 **2.1 Overview**

143 Random replicates of satellite precipitation are generated based on real-time TMPA
144 (3B42RT) retrievals and its uncertainty (Pan et al., 2010), which are then used to force
145 the VIC land surface model (LSM) where one output of interest is surface soil moisture.
146 Satellite soil moisture data products are compared and merged with the 3B42RT product
147 to improve the accuracy of the satellite precipitation estimates. A schematic for the study
148 approach is provided in Figure 1. Based on real-time 3B42RT retrievals, a set of possible
149 precipitation estimates (a.k.a. replicates or particles) $\{p^i\}_{i=1,2,\dots,N}$ is generated with
150 assigned initial prior probability weights $\{w^i\}_{i=1,2,\dots,N}$. These rainfall rates are then used
151 to force the VIC land surface model to produce soil moisture predictions $\{\theta^i\}_{i=1,2,\dots,N}$.
152 Retrievals of AMSR-E satellite surface soil moisture using the Land Surface Microwave
153 Model (LSMEM) (Pan et al., 2014) are then merged with the LSM-based soil moisture
154 within the Particle Filter (PF) that compares AMSR-E/LSMEM changes in soil moisture,
155 ΔSM , to the LSM predicted soil moisture changes. From these, posterior weights
156 $\{w^{i+}\}_{i=1,2,\dots,N}$ are calculated for each precipitation member (particle) that takes into
157 account the uncertainties of AMSR-E/LSMEM ΔSM retrievals. From these updated
158 weights, an updated precipitation probability distribution is constructed, where the
159 precipitation particle with highest probability is taken as the “best” adjusted precipitation
160 estimate ($3B42RT_{ADJ}$). The procedure is carried out over the continental US (CONUS)
161 region on a grid-by-grid basis (0.25-degree) and a daily time step. Allowing for 6 months
162 model spin-up period, the adjustment is done from January 2003 to July 2007.

163 **2.2 Modeling, Statistical Tools and Data Sources**

164 **2.2.1 The Particle Filter**

165 Data assimilation methods are capable of dynamically merging predictions from a state
166 equation (i.e. the land surface model) with measurements (i.e. AMSR-E retrievals) to
167 minimize uncertainties from both the predictions and measurements. It is assumed that

168 the source of uncertainty in the land surface model predictions come solely from the real-
 169 time satellite precipitation, so that the particle filter (PF) provides an algorithm to update
 170 the precipitation based on the AMSR-E retrievals. The state evolution of a particle filter
 171 from discrete time $t-1$ to t can be represented as:

$$172 \quad \theta_t = f_t(\theta_{t-1}, p_t, \kappa_t, \alpha_t) \quad (1)$$

173 where θ_t is the 1st layer soil moisture at time t , whose value is predicted by the state
 174 equation Eq.(1) as $f_t(\bullet)$, and in the study is the hydrological model VIC, which takes in
 175 forcing data, including precipitation (p_t) and other forcings (κ_t); and simulates land
 176 surface states (soil moisture and soil temperatures at various levels, snow, etc.) and fluxes
 177 (evapotranspiration, runoff) at time t . Herein we are basically interested only in the 1st
 178 layer (top 10cm) soil moisture state and precipitation forcing, so other states and fluxes
 179 are not explicitly shown. α_t is the random error in the prediction of θ_t , whose statistics
 180 are known but not its value at any specific time.

181 At time t , the satellite surface soil moisture retrieval, θ_t^* , can be related to the VIC
 182 modeled 1st layer soil moisture θ_t as:

$$183 \quad \theta_t^* = h_t(\theta_t, \beta_t) \quad (2)$$

184 where h_t is taken as a regression that transforms the VIC simulated 1st layer soil
 185 moisture to satellite surface soil moisture. β_t is the noise in this regression relationship.
 186 The two noises α_t and β_t are assumed to be independent of each other at all times t .

187 At time t , given a 3B42RT precipitation estimate, p_t^{sat} , a set of N precipitation replicates
 188 $\{p_t^i\}_{i=1,2,\dots,N}$ and their associated initial prior probability weight $\{w_t^i\}_{i=1,2,\dots,N}$ are
 189 generated.

$$190 \quad g(p_t^{\text{sat}}) \sim \{p_t^i, w_t^i\}_{i=1,2,\dots,N} \quad (3)$$

$$191 \quad \sum_{i=1}^N w_t^i = 1 \quad (4)$$

192 $g(\cdot)$ is a probability density function. For N precipitation replicates, $\{p_t^i\}_{i=1,2,\dots,N}$, the
 193 propagation of the states from time step $(t-1)$ to t is by the VIC land surface model

194 represented in Eq.(1). The VIC land surface model simulates the 10cm 1st layer soil
 195 moisture, $\{\theta_t^i\}_{i=1,2,\dots,N}$ for each precipitation replicate.

$$196 \quad \{\theta_t^i = f_t(\theta_{t-1}, p_t^i, \kappa_t, \alpha_t)\}_{i=1,2,\dots,N} \quad (5)$$

197 with the associated weights assigned to the precipitation member:

$$198 \quad \{\theta_t^i, w_t^i\}_{i=1,2,\dots,N} = \{f_t(\theta_{t-1}, p_t^i, \kappa_t, \alpha_t), w_t^i\}_{i=1,2,\dots,N} \quad (6)$$

199 If the satellite soil moisture retrieval at time t is θ_t^* , the update of precipitation forcing is
 200 accomplished by updating the importance weight of each replicate given the
 201 “measurement” θ_t^* :

$$202 \quad w_t^{i+} \sim \{g(\theta_t^i | \theta_t^*)\}_{i=1,2,\dots,N} \quad (7)$$

$$203 \quad \sum_{i=1}^N w_t^{i+} = 1 \quad (8)$$

204 The likelihood function $g(\theta_t^i | \theta_t^*)$ can be derived from h_t and $g(\beta_t)$. The schematic of the
 205 utilized strategy is shown in Figure 2. The primary disadvantage of the particle filter is
 206 the large number of replicates required to accurately represent the conditional probability
 207 densities of p_t and θ_t . When the measurements exceed a few hundred, the particle filter is
 208 not computationally practical for land surface problems. Considering computation
 209 efficiency, we set the number of independent particles, N, from the prior distribution to
 210 be 200.

211 **2.2.2 Precipitation Replicates Generation**

212 We generate precipitation replicates, $\{p_t^i\}_{i=1,2,\dots,N}$, based on statistics comparing NLDAS
 213 and 3B42RT precipitation, as shown in Figure 3. Given a 3B42RT precipitation
 214 measurement (binned by magnitude), with bin minimum and maximum indicated in
 215 Figure 3, precipitation replicates are generated based on the corresponding 15th, 30th, 70th,
 216 85th percentiles and the maximum NLDAS precipitation of the particular quantile bin as
 217 follows: 15% of the replicates are generated with values uniformly distributed from 0 and
 218 15th percentile; 15% of replicates with values from 15th to 30th percentile; 20% of
 219 replicates with values from 30th percentile to the median; 20% of the replicates generated
 220 from the median to 70th ; 15% with values from 70th to 85th percentile; and 15% from the

221 85th percentile to the maximum precipitation value. Note that although the generation of
222 particles is based on statistics calculated from NLDAS, results show little difference
223 generating precipitation ensembles uniformly distributed between 0 and 200 mm/day.

224 **2.2.3 AMSR-E/LSMEM Soil Moisture Retrievals**

225 The soil moisture product is derived from multiple microwave channels of the Advanced
226 Microwave Scanning Radiometer for EOS (AMSR-E) instrument. The retrieval algorithm
227 by Pan et al. (2014) is an enhanced version of the Land Surface Microwave Emission
228 Model (LSMEM). The near surface soil moisture and vegetation optical depth (VOD) are
229 estimated simultaneously from a dual polarization approach that utilizes both horizontal
230 (H) and vertical (V) polarizations measurement by the space-borne sensor. The input
231 AMSR-E brightness temperature comes from the NSIDC AMSR-E/Aqua Daily Global
232 Quarter-Degree Gridded Brightness Temperatures product (overlapping swaths in the
233 same day are truncated so that only the latest one is present). Consequently, the soil
234 moisture retrievals are also gridded at 0.25-degree with one ascending map and one
235 descending map at the daily time step. A maximum threshold value of $0.6 \text{ m}^3/\text{m}^3$ has been
236 applied manually to reduce error from open water bodies. According to Pan et al. (2014),
237 the soil moisture dataset based on observations from AMSR-E are shown to be consistent
238 at large scales in terms of reproducing the spatial pattern of soil moisture from VIC land
239 surface model simulation. Ascending soil moisture retrievals (equatorial crossing time
240 1:30PM local time) is assimilated in this study.

241 Similarly, while the spatial patterns of the basic statistics of AMSR-E/LSMEM SM
242 retrievals compare well to VIC simulations (Pan et al., 2014), VIC has its top layer (10
243 cm), which is deeper than the detection depth of AMSR-E, so that the mean and temporal
244 variability of the retrievals are higher than the VIC simulated soil moisture (Figure 4 in
245 Pan et al., 2014). Considering this difference between detection depths, we pre-process
246 soil moisture retrievals as follows:

247 1) Rescale soil moisture retrievals (AMSR-E/LSMEM SM) to have the same minimum
248 and maximum range as VIC simulated 1st layer soil moisture.

250 2) Calculate a daily soil moisture change. As satellite retrievals are manually truncated to
251 be no more than $0.6 \text{ m}^3/\text{m}^3$ (equivalent to 60mm of water in the top soil layer in VIC),
252 retrievals larger than $0.6 \text{ m}^3/\text{m}^3$ are excluded.

253 3) Fit a 2nd order polynomial regression model with ΔSM (all units in mm of water in the
254 top layer) from satellite and VIC simulation on a monthly basis and 3×3 grid scale
255 (window).

256 After pre-processing, the distribution of soil moisture change matches fairly well with
257 $\Delta\text{SM}_{\text{VIC}}$ (Figure 4). The mean absolute difference reduces from a spatial average of 5.25
258 mm/day to 0.71 mm/day, with relatively larger value over eastern CONUS. According to
259 Pan et al. (2014), the no-skill or negative-skill areas occur mostly over eastern dense
260 forests due to vegetation blockage of the soil moisture signal (Pan et al., 2014). The
261 accuracy of soil moisture retrievals is also limited by mountainous topography and the
262 occurrence of snow and frozen ground during winter whose identification from satellite
263 observations is often difficult. For the purpose of this study, we assign zero weight to the
264 $3\text{B42RT}_{\text{ADJ}}$ and rely exclusively on the initial 3B42RT precipitation for time steps when
265 the VIC model predicts snow cover or frozen surfaces.

266 **2.2.4 VIC Land Surface Model**

267 The Variable Infiltration Capacity (VIC) model (Liang et al., 1994; Gao et al., 2010) is
268 used to dynamically simulate the hydrological responses of soil moisture to precipitation,
269 surface radiation and surface meteorology. The VIC model solves the full energy and
270 water balance over each 0.25-degree-grid-cell independently, thus ensuring its
271 computational efficiency. The assumption of independency poses limitation on the
272 application of LSM at very high spatial resolution (e.g. $1\text{km}\times 1\text{km}$) over large areas.
273 Three-layer-soil-moisture is simulated through a soil-vegetation-atmosphere transfer
274 (SVAT) scheme, which also accounts for sub-grid scale heterogeneity of vegetation, soil
275 and topography. A detailed soil moisture algorithm description can be found in Liang et
276 al. (1996). The VIC model has been validated extensively over CONUS by evaluating
277 soil moisture and simulations to observations (Robock et al., 2003; Schaake et al., 2004).

278 **3 Idealized Experiment**

279 Before applying the Particle Filter assimilation algorithm on 3B42RT precipitation
280 estimates, we conducted an idealized experiment where we treat the NLDAS
281 precipitation as the “truth” and the NLDAS precipitation forced VIC simulations as
282 “satellite observed” soil moisture. As an idealized experiment, we adjust TMPA real-time
283 precipitation estimates based on these “satellite observations”. Phase 2 of the North
284 American Land Data Assimilation System (NLDAS-2) rainfall forcing combines hourly
285 WSR-88D radar analyses from the National Weather Service (NWS) and daily gauge
286 reports (~13,000/day) from the Climate Prediction Center (CPC) (Ek et al., 2011). The
287 dataset, with a spatial resolution of 0.125 degree and hourly observations, was pre-
288 processed into 0.25-degree daily precipitation to be consistent with that of 3B42RT and
289 AMSR-E/LSMEM SM datasets. Hourly NLDAS and 3-hourly 3B42RT precipitation is
290 aggregated into daily precipitation defined by a period shifted ~7.5 hours into the future
291 (9:00PM-9:00PM), allowing for a necessary delay for soil moisture to respond to
292 incoming rainfall. The idealized experiment is designed to test whether the algorithm is
293 able to retrieve rainfall forcing with soil moisture change, assuming that the soil moisture
294 observations are 100% accurate.

295 Results show that, with the knowledge of 1st layer soil moisture change (via the “satellite
296 observations”), the adjustment is able to recover intensity and spatial pattern of forcing
297 precipitation (Figure 5g). Average mean absolute error (MAE) of daily rainfall amount is
298 reduced by 52.9% (2.91 mm/day to 1.37 mm/day) over the region. Figure 5a to Figure 5e
299 shows an example of the recovered rainfall field from the idealized experiment for 27th
300 Oct. 2003. The spatial pattern matches the original NLDAS precipitation well.

301 **3.1 Effect of surface soil saturation**

302 While successfully recovering the general pattern of NLDAS precipitation based on first
303 layer soil moisture, the idealized experiment is not always able to recover the
304 precipitation volume due to the fact that the top layer soil moisture alone does not contain
305 the complete memory of the previous day’s rainfall. Deeper soil moisture,
306 evapotranspiration and runoff also carry part of this information. As the surface gets

Authors 8/31/2015 3:38 PM
Deleted: Figure 6).

Authors 8/31/2015 3:38 PM
Deleted: 91mm

Authors 8/31/2015 3:38 PM
Deleted: 37mm

310 wetter, the VIC 1st layer soil moisture has smaller variation. If the incoming precipitation
311 brings the surface to saturation, the VIC model redistributes the soil moisture vertically
312 through vertical moisture flow and generates runoff. Hence soil moisture increments,
313 ΔSM , near saturation are less correlated with incoming precipitation as they change
314 minimally to additional incoming rainfall. An example demonstrating this saturation
315 effect is shown in Figure 5f to Figure 5j. When incoming precipitation brings the surface
316 SM to (near) saturation, there is very limited improvement after the adjustment. Because
317 of the low sensitivity of the soil surface to precipitation, there is little change in ΔSM in
318 response to precipitation variations among the replicates. It is almost always the case that
319 the algorithm is not able to find a “matching” ΔSM .

320 We separately evaluate the skill improvement in the recovered NLDAS precipitation with
321 and without surface saturation. [Figure 6 confirms the effect of surface saturation on](#)
322 [adjusted precipitation, which is well described in previous studies \(e.g. Brocca et al.,](#)
323 [2013, 2014\).](#) The recovered precipitation, when the surface soil is saturated, only
324 contributes more noise rather than an improvement to the rainfall estimates. The VIC
325 model computes the moisture flow between soil layers using an hourly time step. If the 1st
326 layer soil moisture exceeds its maximum capacity, it is considered to be a surface
327 saturation case. As seen in Figure 5, there is very limited or negative skill in the
328 recovered precipitation under saturated surface soil moisture conditions. Such
329 circumstances are identified and the AMSR-E/LSMEM ΔSM observation disregarded by
330 assigning zero weight to the 3B42RT_{ADJ} values. Thus for wetter areas with heavy
331 precipitation that potentially would bring the surface soil moisture to saturation, the
332 3B42RT product is less likely to be adjusted according to satellite ΔSM and the best
333 precipitation estimate is 3B42RT.

334 3.2 Effect of SM uncertainty

335 In the idealized experiment, NLDAS-VIC soil moisture is taken as truth with zero
336 uncertainty associated with (θ_t^*). However, this assumption is not valid for real satellite
337 SM retrievals, mean absolute error of which is approximately 3% vol./vol. (McCabe et
338 al., 2005). To consider this, we added error to the “truth” SM (normally distributed with
339 [zero mean and standard deviations of 1mm, 2mm, 3mm, 4mm and 5mm](#)), and simulated

Authors 8/31/2015 3:38 PM
Moved (insertion) [1]

Authors 8/31/2015 3:38 PM
Deleted: (Figure 6).

Authors 8/31/2015 3:38 PM
Deleted: 0.

Authors 8/31/2015 3:38 PM
Deleted: , 1.0mm, 1.5mm, 2.0mm, 2.5mm,
3.0mm, 3.5mm, 4.0mm 4.5mm and 5.0mm

344 the effect of SM uncertainty to evaluate the associated adjustment errors. Figure 7 shows
345 that larger soil moisture observation errors lead to larger error variation after adjustment.
346 This also suggests that soil moisture responds to precipitation non-linearly based on
347 different initial conditions. An estimated wetter surface has lower sensitivity to an
348 incoming rainfall amount, resulting in larger error in the recovered NLDAS precipitation.
349 As shown in Figure 7, the error standard deviation of the recovered NLDAS precipitation
350 increases with surface water content (statistics shown in Table 2). As we add noise larger
351 than $N(0, 1\text{mm})$ into “true” SM observation, there is a wet bias of approximately 1
352 mm/day regardless of 1st layer soil moisture level. This suggests that when the difference
353 between 1st layer SM and saturation is less than 8 mm , the median of the errors in the
354 recovered NLDAS precipitation grows from 0.16 mm/day to 1.89 mm/day when we add
355 $N(0, 5\text{mm})$ noise, while inter-quantile range (IQR) increases from 1.71 mm/day to 7.04
356 mm/day . Acknowledging such a wet bias, to avoid introducing any more unintentional
357 bias in the $3B42RT_{ADJ}$ estimates, we take as zero the uncertainty of AMSR-E/LSMEM
358 SM retrievals, i.e. we take $h_t(\theta_t)$ as our single observation θ_t^* and adjust the $3B42RT$
359 estimates accordingly.

360 It is noteworthy that the soil moisture change is calculated based on previous days’ soil
361 water contents. Therefore errors tend to accumulate over time until they are “re-set” when
362 a significant precipitation event takes place. This type of uncertainty accounts for a small
363 portion of the total error in the adjusted precipitation (black being the no error case in
364 Figure 7 with the “true” change in soil moisture from every time step). As complete
365 global coverage is not provided with each orbit of the AMSR-E sensor, on average 44.01%
366 of the time steps ($<0.6\text{ m}^3/\text{m}^3$) during the study period have observations, with more
367 frequent overpasses at higher latitudes (Figure 4e in Pan et al., 2014). This observation
368 gap unavoidably introduces extra uncertainty in the retrieval of the precipitation signal.
369 To further avoid possible additional errors, we update the forcing rainfall when a ΔSM
370 temporal match ($\pm 0.4\text{mm}$) is available, and keep the original precipitation if a match isn’t
371 available.

Authors 8/31/2015 3:38 PM

Deleted: 0.5mm

Authors 8/31/2015 3:38 PM

Deleted: 1mm

Authors 8/31/2015 3:38 PM

Deleted: 8mm

Authors 8/31/2015 3:38 PM

Deleted: 16mm

Authors 8/31/2015 3:38 PM

Deleted: 89mm

Authors 8/31/2015 3:38 PM

Deleted: 5.0mm

Authors 8/31/2015 3:38 PM

Deleted: 71mm

Authors 8/31/2015 3:38 PM

Deleted: 04mm

380 **4 Improvement on real-time precipitation estimates and their validation**

381 The adjustment of real TMPA 3B42RT retrievals based on AMSR-E/LSMEM ΔSM is
382 carried out using the methods described in Section 2.2.3, and results from the idealized
383 experiment (Sect. 3) with regard to the circumstances where an adjustment is applied.

384 An example of TMPA 3B42RT adjustment is provide in Figure 8, where a snapshot of
385 the rainfall field is shown (Figure 8b) and compared with NLDAS on May 26th 2006 and
386 the adjusted rainfall pattern based on AMSR-E/LSMEM ΔSM. The 3B42RT_{ADJ} rainfall
387 field (Figure 8c) is similar in terms of its spatial distribution compared to NLDAS
388 precipitation estimates (Figure 8d).

389 On average TMPA 3B42RT and AMSR-E/LSMEM ΔSM have a spatial Pearson
390 Correlation Coefficient of 0.37 (Shown in Figure 9, left), compared to 0.52 for the
391 correlation between NLDAS and ΔSM. After the adjustment procedure, the Pearson
392 correlation coefficient between 3B42RT_{ADJ} and AMSR-E/LSMEM ΔSM increases to
393 0.53, (shown in Figure 9), indicating that the correction method is successful. A below
394 average increase in correlation is found over the western mountainous region, the Great
395 Lakes region and eastern high vegetated and populated region. Additionally, the satellite
396 soil moisture suffers from snow/ice/standing water contamination, which affects the
397 potential for improved results after correction. The 3B42RT_{ADJ} has significant
398 improvement over 3B42RT in terms of long-term precipitation bias. The bias in 3B42RT
399 annual mean precipitation is reduced by 20.6%, from -9.32mm/month spatial average in
400 3B42RT to -7.40mm/month in 3B42RT_{ADJ} (shown in Figure 9, right). Frequency of rain
401 days generally increases significantly everywhere, (Figure 10). The NLDAS data (Figure
402 10, right) suggests an almost constant drizzling rainfall over parts of the western
403 mountainous area (Montana, Idaho, Wyoming and Colorado), while assimilating AMSR-
404 E/LSMEM ΔSM datasets does not have a signal of higher rainfall frequency, (Figure 10,
405 middle). This is possibly due to lower soil moisture variability in satellite retrievals over
406 the dry, mountainous areas and frequent presence of snow and ice (3B42RT is not
407 updated under such circumstances).

408 Figure 11 shows the assimilation results for the grids and days with soil moisture
409 observations, using the NLDAS precipitation as a reference. Overall, the method is

- Authors 8/31/2015 3:38 PM
Deleted: Actual
- Authors 8/31/2015 3:38 PM
Deleted: the
- Authors 8/31/2015 3:38 PM
Deleted: Figure 8 shows
- Authors 8/31/2015 3:38 PM
Deleted: from the 3B42RT
- Authors 8/31/2015 3:38 PM
Deleted: product
- Authors 8/31/2015 3:38 PM
Deleted: d).
- Authors 8/31/2015 3:38 PM
Deleted: has
- Authors 8/31/2015 3:38 PM
Deleted: average
- Authors 8/31/2015 3:38 PM
Deleted: Figure.A1
- Authors 8/31/2015 3:38 PM
Deleted: . There
- Authors 8/31/2015 3:38 PM
Deleted: a smaller
- Authors 8/31/2015 3:38 PM
Deleted: adjustment. In general, adjustment decreases rainfall amount while increases rain days (frequency of rainy days shown in Figure 9 and Figure 10).
- Authors 8/31/2015 3:38 PM
Deleted: underestimated
- Authors 8/31/2015 3:38 PM
Deleted: , which
- Authors 8/31/2015 3:38 PM
Deleted: %
- Authors 8/31/2015 3:38 PM
Deleted: Figure.A1
- Authors 8/31/2015 3:38 PM
Deleted: .
- Authors 8/31/2015 3:38 PM
Deleted: .
- Authors 8/31/2015 3:38 PM
Deleted:). The excessive 3B42RT_{ADJ} rainfall events comes from the high-frequency noise in AMSR-E/LSMEM soil moisture retrievals identified by Pan et, al (2004) and Wanders et al. (2015)
- Authors 8/31/2015 3:38 PM
Deleted: Figure 9 presents false alarm rate (FAR) and probability of detection (POD) of 3B42RT and 3B42RT_{ADJ}, using NLDAS as reference dataset. The rain event threshold is set to be 0.1mm/day and 2mm/day. Cor ... [1]

462 successful in correcting daily rainfall amount when 3B42RT overestimates precipitation,
463 $(3B42RT - NLDAS > 0)$. Mean standard deviation (STD) of $3B42RT_{ADJ} - NLDAS$ is
464 between 1 and 3 mm/day (statistics provided in Table 3). When 3B42RT underestimates
465 rainfall, $(3B42RT - NLDAS < 0)$, the assimilation has limited improvement on 3B42RT.
466 This is due to the effect of surface saturation. In terms of adding rainfall, there are two
467 scenarios when the effectiveness of the assimilation is limited.

468 1) The presence of wet conditions or (near) saturation. There is higher probability
469 bringing the surface to saturation (wetter condition) when the assimilation adds
470 rainfall into 3B42RT. However soil moisture increments are less sensitive to
471 incoming precipitation on wetter soil. Therefore, an error in ΔSM often translates into
472 $3B42RT_{ADJ}$ in a magnified manner.

473 2) The presence of very heavy precipitation, which typically brings the surface to
474 saturation, hence not results in an update of 3B42RT, is not updated. If, by a small
475 probability, the surface is wet (nearly saturated) but not completely saturated after a
476 heavy rainfall, the updated 3B42RT also suffers from large uncertainty (explained in
477 1) above).

478 The effect of the assimilation conditioned on 3B42RT rainfall amount is further evaluated,
479 by skill scores. Figure 12 presents probability of detection (POD) and false alarm rate
480 (FAR) in 3B42RT and $3B42RT_{ADJ}$, using NLDAS as the reference dataset. The rain event
481 threshold is set to be 0.1 mm/day and 2 mm/day. This is possibly due to lower soil
482 moisture variability in satellite retrievals over the dry, mountainous areas and frequent
483 presence of snow and ice (3B42RT is not updated under such circumstances). For a 0.1
484 mm/day threshold, both FAR and POD increases in $3B42RT_{ADJ}$ except for the
485 mountainous region. Whereas for a 2 mm/day threshold, there is only slight increase in
486 FAR in most of eastern U.S. region. The overestimation of rain days is also absent when
487 2 mm/day event threshold is applied which suggests that most of the excessive rainy days
488 have less than 2 mm/day rain amount. Consistent with other studies, spatially, larger
489 improvements are found in the central U.S. The area coincides where higher AMSR-
490 E/LSMEM ΔSM accuracy is found (non-mountainous regions with little urbanization and
491 light vegetation). Despite of the regional variability, these excessive rainy days are a

Authors 8/31/2015 3:38 PM

Deleted: .

Authors 8/31/2015 3:38 PM

Deleted: 3mm

Authors 8/31/2015 3:38 PM

Deleted: .

Authors 8/31/2015 3:38 PM

Deleted: a ΔSM

Authors 8/31/2015 3:38 PM

Deleted: to

Authors 8/31/2015 3:38 PM

Deleted: near

Authors 8/31/2015 3:38 PM

Deleted: a

Authors 8/31/2015 3:38 PM

Deleted: Since the prior knowledge of overestimated precipitation is not always available, the

Authors 8/31/2015 3:38 PM

Deleted: .

503 [result of the high-frequency noise in AMSR-E/LSMEM soil moisture retrievals identified](#)
504 [by Pan et al \(2004\) and Wanders et al. \(2015\).](#)

505 The applied method is ineffective for light rainfall [\(< 2 mm\)](#), where the adjustment tends to
506 over-correct precipitation by adding excessive rainfall – [mostly the result of the high](#)
507 [frequency AMSR-E noise. MAE of light rainfall \(< 2 mm/day\) increased from 0.65](#)
508 [mm/day in 3B42RT to 0.99 mm/day in 3B42RT_{ADJ}.](#) On the other hand, [satellite soil](#)
509 [moisture assimilation is very effective in correcting satellite precipitation larger than 2](#)
510 [mm/day: MAE of medium to large rainfall \(≥ 2 mm/day\) decreased from 7.07 mm/day in](#)
511 [3B42RT to 6.55 mm/day in 3B42RT_{ADJ}.](#) The effect of [the](#) assimilation is different over
512 the western mountainous region, the north-to-south central U.S. band and the eastern U.S.

513 The western mountainous region has a dry climatology with more frequent rainfall in
514 small [amounts](#). The white noise [in ΔSM](#), negatively impacting 3B42RT_{ADJ}, is comparable
515 to the positive improvement brought by [actual](#) light rainfall signals in ΔSM. Therefore,
516 the assimilation of ΔSM has no significant impact [in these regions](#).

517 The north-to-south band over central U.S. experiences more medium [to large \(≥ 2](#)
518 [mm/day\)](#) rainfall. In addition, the region is lightly vegetated (annual mean LAI <1) with
519 low elevation ([< 1500 m](#)), where soil moisture retrievals are of higher accuracy. Soil
520 moisture climatology is wetter [in](#) the west, causing larger [variations](#) in 3B42RT_{ADJ} error
521 from the white noise ΔSM (as discussed in Section 3.2). Despite of that, satellite soil
522 moisture is most effective correcting medium to large rainfall [under](#) normal surface
523 [conditions](#).

524 The decreased skill in 3B42RT_{ADJ} over eastern U.S. is primarily attributed to both
525 precipitation and soil moisture climatology, [a](#) wet climate with more medium to large
526 rainfall, neither of which is suitable for soil moisture assimilation.

527 In summary, the high-frequency noise in soil moisture product [causes](#) a major limitation.
528 The noise impacts adjusted precipitation by introducing false alarm [rain](#) days. It is
529 difficult to distinguish the noise and [retrieve the](#) true rainfall signals. A remedy [to prevent](#)
530 the excessive [rain](#) days is applying a cutoff ΔSM threshold when [rain](#) days are added, at
531 the expense of neglecting a part of the true rainfall signals. [Figure 13 shows the](#)
532 [probability of added rainy days being consistent with NLDAS \(NLDAS > 0 mm/day\)](#)

Authors 8/31/2015 3:38 PM
Deleted: <2mm

Authors 8/31/2015 3:38 PM
Deleted: coming

Authors 8/31/2015 3:38 PM
Deleted: the high frequency AMSR-E noise.

Authors 8/31/2015 3:38 PM
Deleted: Satellite

Authors 8/31/2015 3:38 PM
Deleted: of larger than 2mm/day.

Authors 8/31/2015 3:38 PM
Deleted: amount. Skills are limited by the white noise in ΔSM.

Authors 8/31/2015 3:38 PM
Deleted: real

Authors 8/31/2015 3:38 PM
Deleted: (

Authors 8/31/2015 3:38 PM
Deleted: -20mm

Authors 8/31/2015 3:38 PM
Deleted: 1500m

Authors 8/31/2015 3:38 PM
Deleted: than

Authors 8/31/2015 3:38 PM
Deleted: variation

Authors 8/31/2015 3:38 PM
Deleted: with

Authors 8/31/2015 3:38 PM
Deleted: condition

Authors 8/31/2015 3:38 PM
Deleted: is

Authors 8/31/2015 3:38 PM
Deleted: rainy

Authors 8/31/2015 3:38 PM
Deleted: of

Authors 8/31/2015 3:38 PM
Deleted: rainy

Authors 8/31/2015 3:38 PM
Deleted: rainy

Authors 8/31/2015 3:38 PM
Deleted: By comparing the distribution

554 [with respect to \$\Delta SM\$. When a new rainy day is added \(\$3B42RT = 0\$ mm/day, \$3B42RT_{ADJ}\$](#)
 555 [\$> 0\$ mm/day\) based on AMSR-E/LSMEM \$\Delta SM\$ of \$2\$ mm/day, there's approximately 78%](#)
 556 [chance that the added rain day is a true event \(NLDAS \$> 0\$ mm/day\); That is, approx.](#)
 557 [22% chance that it is a false alarm \(NLDAS = \$0\$ mm/day\). When AMSR-E/LSMEM](#)
 558 [\$\Delta SM\$ is larger than \$2\$ mm/day, the probability of added rainy days being true event is](#)
 559 [even higher, up to 90% chance. Here we applied a threshold of \$2\$ mm/day on AMSR-](#)
 560 [E/LSMEM \$\Delta SM\$. That is, when new rainy days are introduced \(\$3B42RT > 0\$,](#)
 561 [\$3B42RT_{ADJ} > 0\$ \), we discard the update and keep the no-rain day if AMSR-E/LSMEM](#)
 562 [soil moisture increment is below \$2\$ mm. Note that, the probability of the false alarms](#)
 563 [depends on soil moisture climatology: the wetter soil moisture climatology, the larger](#)
 564 [uncertainty in the signal. Therefore, this threshold should vary in accordance with local](#)
 565 [soil moisture climatology, i.e. a larger threshold over the wetter east U.S. and smaller](#)
 566 [threshold over the drier western U.S. Nevertheless, after the \$2\$ mm/day \$\Delta SM\$ threshold is](#)
 567 [applied, expectedly, the statistics are largely improved: FAR is decreased significantly](#)
 568 [from \$0.519\$ \(w.o. \$\Delta SM\$ threshold\) to \$0.066\$ \(w. \$\Delta SM\$ threshold\). MAE of light rainfall \(\$< 2\$](#)
 569 [mm/day\) in \$3B42RT_{ADJ}\$ decreased from \$0.99\$ mm/day to \$0.64\$ mm/day, compared to \$0.65\$](#)
 570 [mm/day in \$3B42RT\$. For medium to large \$3B42RT\$ rainfall \(\$\geq 2\$ mm/day\), it effectively](#)
 571 [increased POD \(\$0.362\$ in \$3B42RT\$ vs \$0.386\$ in \$3B42RT_{ADJ}\$ w. \$\Delta SM\$ threshold\) and](#)
 572 [decreased FAR \(\$0.037\$ in \$3B42RT\$ vs \$0.030\$ in \$3B42RT_{ADJ}\$ w. \$\Delta SM\$ threshold\). Further](#)
 573 [work is needed to characterize, distinguish and decrease the high-frequency noise in SM](#)
 574 [retrievals. Figure 13 gives an example of evaluating the impact of SM uncertainties in](#)
 575 [assimilation as curves derived over different topography can be quantitatively compared.](#)

576 **5 Comparison to other studies**

577 Many other studies have [utilized satellite microwave brightness temperatures or soil](#)
 578 [moisture retrievals to constrain satellite precipitation estimates \(Pellarin et al., 2008\),](#)
 579 [estimate precipitation \(e.g. Brocca et al., 2013\) or improve precipitation estimates,](#)
 580 [through assimilation \(Crow et al., 2009, 2011\). Here, we review their approaches and](#)
 581 [findings in light of the results of this study, and compare our results with some of these](#)
 582 [studies to gain insight into their robustness and consistency.](#)

Authors 8/31/2015 3:38 PM
 Deleted: ΔSM

Authors 8/31/2015 3:38 PM
 Deleted: falsely reported in $3B42RT_{ADJ}$, a cutoff ΔSM threshold of 2 mm/day could filter out 99.8% of the false alarms. The simple application of a spatially uniform, stationary cutoff ΔSM threshold on the added rainy days could distinguish 3.3% of the true rain signals. The same evaluation metrics for

Authors 8/31/2015 3:38 PM
 Deleted: after cutoff threshold is applied are provided in Figure 12c-d. Expectedly, the statistics are largely improved.

Authors 8/31/2015 3:38 PM
 Formatted: Not Superscript/ Subscript

Authors 8/31/2015 3:38 PM
 Deleted: rain amount

Authors 8/31/2015 3:38 PM
 Deleted: Intensity-duration-frequency curves are also shown in Figure.A 2. Again, the difference in the performance of adjusted rainfall of selected grids is associated with local climatology. Thus

Authors 8/31/2015 3:38 PM
 Deleted: However, it should also be noted that the application of the cutoff

Authors 8/31/2015 3:38 PM
 Deleted: is not able to decrease uncertainties for

Authors 8/31/2015 3:38 PM
 Deleted: .

Authors 8/31/2015 3:38 PM
 Deleted: analyzed the assimilation of

Authors 8/31/2015 3:38 PM
 Deleted: to

Authors 8/31/2015 3:38 PM
 Deleted: . In the following

Authors 8/31/2015 3:38 PM
 Deleted: qualitatively

Authors 8/31/2015 3:38 PM
 Deleted: Our results confirm

Authors 8/31/2015 3:38 PM
 Moved up [1]: the effect of surface saturation on adjusted precipitation, which is well described in previous studies (e.g. Brocca et al.,

Authors 8/31/2015 3:38 PM
 Deleted: 2011, 2013).

615 [Pellarin et al. \(2008\)](#) used the temporal variations of the AMSR-E 6.7 GHz brightness
616 [temperature \(TB\) normalized polarization difference, \$PR=\(TB_V-TB_H\)/\(TB_V+TB_H\)\$, to](#)
617 [screen out anomalous precipitation events from a 4-day cumulative satellite-estimated](#)
618 [precipitation \(EPSAT-SG: Chopin et al., 2005\) from 22 to 26 of June 2004 over a 100 x](#)
619 [125 km box centered over Niger in west Africa. This was extended in Pellarin et al.](#)
620 [\(2013\) where an API-based water balance model was used to correct three different](#)
621 [satellite precipitation products \(CMORPH, TRMM-3B42 and PERSIANN\) over a 4-year](#)
622 [period in west Africa at three 0.25° grids in Niger, Benin and Mali\). The new algorithm](#)
623 [was evaluated by comparing the corrected precipitation to estimates over the 0.25° grids](#)
624 [from ground-based precipitation measurements. A sequential assimilation approach was](#)
625 [applied where AMSR-E C-band TB measurements were used to estimate a simple](#)
626 [multiplicative factor to the precipitation estimates in order to minimize the difference](#)
627 [between observed \(AMSR-E\) and simulated TBs in term of root mean square error](#)
628 [\(RMSE\). The results show improvements over those found in Pellarin et al. \(2009\).](#)
629 [Specifically, the Pellarin et al. \(2013\) study shows that the proposed methodology](#)
630 [produces an improvement of the RMSE at daily, decadal and monthly time scales and at](#)
631 [the three locations. For instance, the RMS mean error decreases from 7.7 to 3.5 mm/day](#)
632 [at the daily time scale in Niger and from 18.3 to 7.7 mm/day at the decadal time scale in](#)
633 [Mali.](#)

634 [Crow et al. \(2003, 2009, 2011\) demonstrated the effectiveness of the assimilation of](#)
635 [remotely sensed microwave brightness temperatures or retrieved soil moisture in](#)
636 [estimating precipitation based on airborne measurements over the Southern Great Plains](#)
637 [\(USA\) region \(Crow et al., 2003\); 2 to 10 day accumulated precipitation within a simple](#)
638 [API water budget model and assimilation scheme over CONUS \(Crow et al., 2009\); and](#)
639 [3 day, 1° precipitation accumulation over three African Monsoon Multidisciplinary](#)
640 [Analysis \(AMMA\) sites in west Africa with an enhanced assimilation scheme and an](#)
641 [API-moisture model \(Crow et al., 2011\). Crow et al. \(2009\) recommends against](#)
642 [estimating precipitation at a larger scale than three days based on assimilating AMSR-](#)
643 [E/LSMEM soil moisture.](#)

644 [Brocca et al. \(2013\) estimated precipitation by inverting the water budget equation such](#)
645 [that precipitation could be estimated from changes in soil moisture. The inverted equation](#)

Authors 8/31/2015 3:38 PM

Deleted: In particular, Wanders et al. (2015, hereby W15) performed a comprehensive study using multiple satellite soil moisture (AMSR-E/LSMEM, ASCAT and SMOS) and land surface temperature data. This study focused exclusively on the usefulness of soil moisture product and differs in the pre-processing method (CDF-matching versus polynomial regression), the temporal period (2010-2011 versus 2002-2007) and the temporal resolution (3-hourly versus da... [2]

658 [was calibrated using in-situ, 4-day averaged observations at two sites in Spain and Italy.](#)
659 [In Brocca et al. \(2014\), the same approach was used globally for 5-day precipitation](#)
660 [totals and at 1° spatially. Soil moisture observations from three satellite derived soil](#)
661 [moisture datasets \(AMSR-E LPRM, ASCAT and SMOS\) were used. The soil moisture](#)
662 [and rainfall were aggregated to a 1° spatial resolution, the soil moisture changes over a 5-](#)
663 [day period to estimate a 5-day total precipitation. No formal data assimilation was carried](#)
664 [out. The newly created precipitation data set was compared to two satellite precipitation](#)
665 [products \(TRMM-3B42RT, GPCC\) and two gauge based precipitation products \(GPCP,](#)
666 [ERA-Interim\). But they do note that their approach has “poor scores in reproducing daily](#)
667 [rainfall data”. Nonetheless, these studies show promising results.](#)

668 [In the study reported here, three advances have been made over these earlier studies: \(i\)](#)
669 [we adopted a state-of-the-art dynamic land surface model that has demonstrated high skill](#)
670 [in simulating soil moisture when driven by high quality precipitation data \(Schaake et al.,](#)
671 [2004\); \(ii\) we applied a state-of-the-art data assimilation procedure based on particle](#)
672 [filtering so as to extract \(and hopefully maximize\) the information content from the](#)
673 [satellite most effectively; \(iii\) we increased the resolution of the precipitation estimation](#)
674 [window down to 1 day, exceeding the conclusions in these earlier studies that the finest](#)
675 [temporal resolution is 3 to 5 days. Additionally we increased \(or matched\) the spatial](#)
676 [resolution to 0.25°, limited primarily by the satellite soil moisture product resolution; and](#)
677 [\(iv\) previous studies are based on the assumption that the SM retrievals are 100%](#)
678 [accurate and contain no errors. We evaluated this assumption by analyzing the impact of](#)
679 [uncertainties associated with the soil moisture retrievals. These advances offer important](#)
680 [benefits when satellite precipitation products are used for applications such as flood](#)
681 [forecasting. Admittedly by aggregating in space and time, the improvement is more](#)
682 [robust since some errors are averaged out. However improving satellite precipitation by](#)
683 [AMSR-E/LSMEM SM is not entirely without skill. In fact, it could effectively correct](#)
684 [rainfall with proper cautions given to local climatology where the assimilation is carried](#)
685 [out.](#)

686 [Wanders et al. \(2015\) performed a comprehensive inter-comparison study using multiple](#)
687 [satellite soil moisture and land surface temperature \(LST\) data at fine temporal scale \(3-](#)
688 [hourly\). Compared to their study, ours focuses on using soil moisture exclusively from](#)

689 [one satellite and retrieval algorithm, and in improvements to the assimilation algorithm.](#)
690 [Specifically in \(i\) the longer temporal period \(2010-2011 in Wanders, et al. versus 2002-](#)
691 [2007 in this study\), \(ii\) the temporal resolution \(3-hourly versus daily\); \(iii\) the particle](#)
692 [generation and bias correction method. We present in the paper improvements in the](#)
693 [generation of rain particles and the bias-correction of the satellite soil moisture](#)
694 [observations, as well as enhancements to the assimilation algorithm to maximize the](#)
695 [information that can be gained from using soil moisture alone in adjusting precipitation.](#)
696 [Due to the very strong and complicated spatial structure of precipitation, that is non-](#)
697 [Gaussian and non-stationary in both time and space, a more advanced method is applied](#)
698 [to generate possible precipitation fields than used or presented in earlier studies or in](#)
699 [Wanders et al, \(2015\). Furthermore, a more advanced bias correction method is also](#)
700 [applied to account for the reported problems \(Wanders et al., 2015\) in the second order](#)
701 [statistics of the soil moisture retrievals; and \(iv\) SM retrieval products \(and overpasses\)](#)
702 [used in assimilation. Our improved results are based on soil moisture retrievals from](#)
703 [ascending overpasses only \(versus both descending and ascending overpasses from](#)
704 [multiple datasets, i.e. AMSR-E/LSMEM, ASCAT and SMOS\). Our exclusive focus on](#)
705 [the usefulness of soil moisture product promises more applicability especially for](#)
706 [improving satellite precipitation from the Global Precipitation Mission products. The](#)
707 [descending overpasses have generally better performance than the ascending, suggesting](#)
708 [the potentials of further improvements.](#)

709 [A quantitative comparison of Wanders et al. \(2015\) and our results is provided below.](#)
710 [Despite of the different time periods between Wanders et al. \(2015, 2010-2011\) and in](#)
711 [our study \(2002-2007\), Wanders et al. \(2015\) shows decreasing POD \(-15.0% to -46.4%](#)
712 [depending on different products used\) and FAR \(-47.2% to -89.1% depending on](#)
713 [different products used\) for all rainfall after assimilation, using either \(single or multiple\)](#)
714 [SM products alone or SM + LST data combined \(see Table 4 of Wanders et al., 2015\).](#)
715 [While in our study, after applying \$\Delta\$ SM threshold, medium to large 3B42RT_{ADJ} rainfall](#)
716 [\(\$\geq 2\$ mm/day\) has an increase in POD \(+6.6%\) and decrease in FAR \(-18.9%\).](#)
717 [Furthermore, the significant dry bias in adjusted precipitation \(see Fig.6 of Wanders et](#)
718 [al., 2015\) is not present in our results \(Figure 9\). This is due to improvements in our](#)
719 [precipitation ensemble generation, and bias correction scheme. Wanders et al. \(2015\)](#)

Authors 8/31/2015 3:38 PM
Formatted: Normal, No bullets or numbering

Authors 8/31/2015 3:38 PM
Deleted: ; however, W15

Authors 8/31/2015 3:38 PM
Deleted: and FAR

Authors 8/31/2015 3:38 PM
Deleted: .

Authors 8/31/2015 3:38 PM
Deleted: . W15

724 applied an additional step generating precipitation particles sampling from a 3×3 window,
 725 that over-eliminates most of the excessive rainfall, along with some real signal. We
 726 suggest loosening this constraint to a larger window size or to sample from adjusted
 727 precipitation instead of original 3B42RT precipitation. However sampling from adjusted
 728 precipitation at each time step, would significantly increase the computational demand,
 729 limiting the potential for a global application at high temporal/spatial resolution.

730 Furthermore, the outcome is quite different for the distribution of soil moisture retrievals
 731 after pre-processing (Fig.9 of Wanders et al. 2015 vs Figure 4 in our study) due to
 732 different methods used. After pre-processing, distributions of soil moisture retrievals is
 733 more similar to that of NLDAS precipitation forced, VIC modeled 1st layer soil moisture.
 734 CDF-matching used by Wanders et al., (2015) is based on the assumption that satellite
 735 soil moisture and modeled soil moisture respond to heavy rainfall in the same way, –
 736 essentially having a rank correlation of 1. However that is not observed because of
 737 shallower detection depth of the satellite soil moisture. On the other hand, using the pre-
 738 processing method presented in this study, the signal of near-saturation in AMSR-
 739 E/LSMEM Δ SM tends to be overestimated after pre-processing, which indicates a heavy
 740 rain event that is often accompanied with surface saturation, and thus does not provide
 741 effective information for the assimilation. The other benefit of the 2nd order polynomial
 742 regression lies in its non-linearity. An error in the soil moisture product impacts the
 743 precipitation adjustment in a predictable way, allowing for a more systematic post-
 744 processing treatment. Based on the known error characteristics, we demonstrate a
 745 potential remedy to deal with the error by applying a 2 mm/day cutoff Δ SM threshold.
 746 Meanwhile, it is also highlighted that the cutoff threshold should be variable and
 747 positively correlated with local soil moisture climatology. We acknowledge that the soil
 748 moisture product used in Wanders et al. (2015), is a blended product of multiple satellite
 749 soil moisture datasets. It is not clear how its error characteristics impact the adjusted
 750 precipitation.

751 6 Conclusion and Discussion

752 Based on the retrieved soil moisture from AMSR-E using the LSMEM retrieval
 753 algorithm, we propose an assimilation procedure to integrate soil moisture information

Authors 8/31/2015 3:38 PM

Deleted: , which effectively filtered out

Authors 8/31/2015 3:38 PM

Deleted: . Note that applying such

Authors 8/31/2015 3:38 PM

Deleted: method, the independence of grid cells in VIC model is no longer maintained. This means that all grids need to be channeled after

Authors 8/31/2015 3:38 PM

Deleted: . Channeling grid cells

Authors 8/31/2015 3:38 PM

Deleted: computation efficiency

Authors 8/31/2015 3:38 PM

Deleted: when applying 0.1mm/day and 2mm/day event threshold (no significant increase in FAR for 2mm/day threshold); While in W15, decrease in both POD and FAR for 0mm/3hr and 2mm/3hr rain event threshold is reported. This is most likely due to the pre-processing method. CDF-matching

Authors 8/31/2015 3:38 PM

Deleted: .

Authors 8/31/2015 3:38 PM

Deleted: true

Authors 8/31/2015 3:38 PM

Deleted: ,

Authors 8/31/2015 3:38 PM

Deleted: in

Authors 8/31/2015 3:38 PM

Deleted: Error

Authors 8/31/2015 3:38 PM

Deleted: proper

Authors 8/31/2015 3:38 PM

Deleted: demonstrated

Authors 8/31/2015 3:38 PM

Deleted: 2mm

Authors 8/31/2015 3:38 PM

Deleted: W15

Authors 8/31/2015 3:38 PM

Deleted: model

779 into the VIC land surface model so as to improve real-time, satellite precipitation
780 estimates. The ability to estimate rainfall amount is now enhanced with the above
781 improvements, especially for [correcting](#) medium rainfall amounts. However, constrained
782 by the noise in [AMSR-E TBs and thus](#) soil moisture retrievals, the assimilation is not
783 effective in detecting missed rainfall events. The improved precipitation estimates,
784 referred to as 3B42RT_{ADJ} estimates, are overall consistent in reproducing the spatial
785 pattern and time series of daily rainfall from NLDAS precipitation. The results illustrate
786 the potential benefits of using data assimilation to merge satellite retrievals of surface soil
787 moisture into a land surface model forced with real-time precipitation. Potentially the
788 method can be applied globally for areas meeting vegetation cover and surface condition
789 constraints that allows for soil moisture retrievals. Under these conditions, the approach
790 can provide a supplementary source of information for enhancing the quality of satellite
791 rainfall estimation, especially over poorly gauged areas like Africa.

Authors 8/31/2015 3:38 PM

Deleted: correction

792 Nonetheless, some caution is required. The results of this study [show](#) that the adjusted
793 real-time precipitation tends to add additional rain (frequency) resulting in more time
794 steps with rain but lower regional average in the [western U.S.](#) and slightly higher regional
795 average in [the](#) eastern U.S. It is also noticed that the precipitation adjustments are
796 insensitive [under](#) saturated soil moisture conditions. A wetter surface magnifies any error
797 associated with satellite observation by incorrectly adjusting precipitation. These errors,
798 mixed with the “real” signal, generally add approximately ~2mm of precipitation (or
799 higher) depending on the soil moisture climatology. It is important to consider these
800 circumstances when observations are used so as to avoid introducing additional error.
801 With these identified limitations, continued research is needed to assess the biases in the
802 real-time precipitation retrievals on a local to regional basis so the assimilation system
803 can be modified accordingly.

Authors 8/31/2015 3:38 PM

Deleted: shows

Authors 8/31/2015 3:38 PM

Deleted: West

Authors 8/31/2015 3:38 PM

Deleted: with

804 The assimilation scheme used here assumed that the errors were attributed to the real-
805 time precipitation retrievals, but the precipitation estimates after adjustment includes
806 errors from additional sources. The two primary sources are errors in soil moisture
807 retrievals and errors in the land surface model that include model parameterizations
808 (poorly or insufficiently represented processes as well as scale issues) and parameter
809 errors (insufficient calibration). There are also errors in other model forcing fields besides

814 precipitation. Further studies are needed to assess the attribution of these error sources to
815 the total error. Such research will further improve the use of real-time satellite-based
816 precipitation for global flood monitoring.

817 Besides the clear, heavy dependency of the assimilation effectiveness on the accuracy of
818 satellite soil moisture product, it is also important to acquire adequate knowledge on the
819 error characteristics of satellite soil moisture retrievals. Knowledge [of the soil moisture](#)
820 [errors](#) could be important and the assimilation methods (including precipitation ensemble
821 generation and pre-/post-processing method) should be chosen accordingly. On the other
822 hand, the presence of data gaps between overpasses could be a large source of uncertainty
823 [with](#) data assimilation. Further effort towards reliable spatial-temporal continuous (gap
824 filled) satellite soil moisture datasets is needed.

825 While it has been illustrated in this study that the enhancement of real time satellite
826 precipitation estimates can be realized through an assimilation approach using satellite
827 soil moisture data products and a particle filter, additional satellite-based observations
828 (e.g. multi-sensor soil moisture products) or variables (e.g. land surface temperatures as
829 shown in Wanders et al. 2015, inundated [areas](#)), could be added/replaced in the
830 assimilation process with different levels of complexity; e.g. [by applying constraints](#) on
831 [the](#) particle generation. This opens up a great number of opportunities in using space-
832 borne observations for supplementing direct retrievals of precipitation.

833 Acknowledgements

834 This research was supported through NASA grant NNX13AG97G (Multi-sensor
835 enhancement of real-time satellite precipitation retrievals for improved drought
836 monitoring) under the Precipitation Measurement Mission. [Part of this research was](#)
837 [financially supported by NWO Rubicon 825.15.003](#). This support is gratefully
838 acknowledged.

839

Authors 8/31/2015 3:38 PM

Deleted: on

Authors 8/31/2015 3:38 PM

Deleted: error

Authors 8/31/2015 3:38 PM

Deleted: in

Authors 8/31/2015 3:38 PM

Deleted: area

Authors 8/31/2015 3:38 PM

Deleted: apply constrains

Authors 8/31/2015 3:38 PM

Formatted: English (UK)

Authors 8/31/2015 3:38 PM

Deleted: Page Break

847 **References**

848 Brocca, L., Melone, F., Moramarco, T. and Morbidelli, R.: Antecedent wetness
849 conditions based on ERS scatterometer data, *J. Hydrol.*, 364(1-2), 73–87,
850 doi:10.1016/j.jhydrol.2008.10.007, 2009.

851 Brocca, L., Moramarco, T., Melone, F. and Wagner, W.: A new method for rainfall
852 estimation through soil moisture observations, *Geophys. Res. Lett.*, 40(5), 853–858,
853 doi:10.1002/grl.50173, 2013.

854 Brocca, L., Ciabatta, L., Massari, C., Moramarco, T., Hahn, S., Hasenauer, S., Kidd, R.,
855 Dorigo, W., Wagner, W. and Levizzani, V.: Soil as a natural rain gauge: Estimating
856 global rainfall from satellite soil moisture data, *J. Geophys. Res. Atmos.*, 119(9), 5128–
857 5141, doi:10.1002/2014JD021489, 2014.

858 | [Chopin, F., Berges, J., Desbois, M., Jobard, I. and Lebel, T.: Satellite Rainfall Probability
859 and Estimation. Application to the West Africa During the 2004 Rainy Season, AGU
860 Spring Meet. Abstr., A12, 2005.](#)

861 Crow, W. T.: Correcting land surface model predictions for the impact of temporally
862 sparse rainfall rate measurements using an ensemble Kalman filter and surface brightness
863 temperature observations, *J. Hydrometeorol.*, 4(5), 960–973, 2003.

864 Crow, W. T., Huffman, G. J., Bindlish, R. and Jackson, T. J.: Improving Satellite-Based
865 Rainfall Accumulation Estimates Using Spaceborne Surface Soil Moisture Retrievals, *J.*
866 *Hydrometeorol.*, 10(1), 199–212, doi:10.1175/2008JHM986.1, 2009.

867 Crow, W. T., Van Den Berg, M. J., Huffman, G. J. and Pellarin, T.: Correcting rainfall
868 using satellite-based surface soil moisture retrievals: The Soil Moisture Analysis Rainfall
869 Tool (SMART), *Water Resour. Res.*, 47(8), 1–15, doi:10.1029/2011WR010576, 2011.

870 | [Dee, D. P., Uppala, S. M., Simmons, A. J., Berrisford, P., Poli, P., Kobayashi, S., Andrae,
871 U., Balmaseda, M. A., Balsamo, G., Bauer, P. and others: The ERA-Interim reanalysis:
872 Configuration and performance of the data assimilation system, *Q. J. R. Meteorol. Soc.*,
873 \[137\\(656\\), 553–597, 2011.\]\(#\)](#)

874 Ebert, E. E., Janowiak, J. E. and Kidd, C.: Comparison of near-real-time precipitation
875 estimates from satellite observations and numerical models, *Bull. Am. Meteorol. Soc.*,
876 88(1), 47–64, doi:10.1175/BAMS-88-1-47, 2007.

877 Ek, M. B., Xia, Y., Wood, E., Sheffield, J., Luo, L., Lettenmaier, D., Livneh, B., Mocko,
878 D., Cosgrove, B., Meng, J., Wei, H., Koren, V., Schaake, J., Mo, K., Fan, Y. and Duan,
879 Q.: North American Land Data Assimilation System Phase 2 (NLDAS-2): Development
880 and Applications, *GEWEX Newsl.*, 21(2), 5–7, 2011.

881 Francois, C., Quesney, A. and Ottlé, C.: SAR Data into a Coupled Land Surface–
882 Hydrological Model Using an Extended Kalman Filter, *J. Hydrometeorol.*, 4(2), 473–487,
883 doi:10.1175/1525-7541(2003)4<473:SAOESD>2.0.CO;2, 2003.

884 Gao, H., Tang, Q., Shi, X., Zhu, C., Bohn, T. J., Su, F., She eld, J., Pan, M., and Wood,
885 E. F.: Water budget record from Variable Infiltration Capacity (VIC) model, in:
886 Algorithm Theoretical Basis Document for Terrestrial Water Cycle Data Records (in
887 review), 2010.

888 Huffman, G. J., Bolvin, D. T., Nelkin, E. J., Wolff, D. B., Adler, R. F., Gu, G., Hong, Y.,
889 Bowman, K. P. and Stocker, E. F.: The TRMM Multisatellite Precipitation Analysis
890 (TMPA): Quasi-Global, Multiyear, Combined-Sensor Precipitation Estimates at Fine
891 Scales, *J. Hydrometeorol.*, 8(1), 38–55, doi:10.1175/JHM560.1, 2007.

892 Huffman, G. J., Adler, R. F., Bolvin, D. T., and Nelkin, E. J.: The TRMM Multi-satellite
893 Precipitation Analysis (TMPA), in: *Satellite Rainfall Applications for Surface*
894 *Hydrology*, Springer Netherlands, 3–22, 2010.

895 Kalman, R. E.: A New Approach to Linear Filtering and Prediction Problems, *J. Basic*
896 *Eng.*, 82(1), 35, doi:10.1115/1.3662552, 1960.

897 [Kerr, Y. H., Waldteufel, P., Richaume, P., Wigneron, J.-P., Ferrazzoli, P., Mahmoodi, A.,](#)
898 [Al Bitar, A., Cabot, F., Gruhier, C., Juglea, S. E., Leroux, D., Mialon, A. and Delwart, S.:](#)
899 [The SMOS Soil Moisture Retrieval Algorithm, *Geosci. Remote Sensing, IEEE Trans.*,](#)
900 [50\(5\), 1384–1403, doi:10.1109/TGRS.2012.2184548, 2012.](#)

901 Liang, X., Lettenmaier, D. P., Wood, E. F. and Burges, S. J.: A simple hydrologically
902 based model of land surface water and energy fluxes for general circulation models, *J.*
903 *Geophys. Res.*, 99, 14415–14428, doi:10.1029/94JD00483, 1994.

904 Liang, X., Wood, E. F. and Lettenmaier, D. P.: Surface soil moisture parameterization of
905 the VIC-2L model: Evaluation and modification, *Glob. Planet. Change*, 13(1-4), 195–
906 206, doi:10.1016/0921-8181(95)00046-1, 1996.

907 Massari, C., Brocca, L., Moramarco, T., Tramblay, Y. and Didon Lescot, J.-F.: Potential
908 of soil moisture observations in flood modelling: estimating initial conditions and
909 correcting rainfall, *Adv. Water Resour.*, 74, 44–53, doi:10.1016/j.advwatres.2014.08.004,
910 2014.

911 Matgen, P., Fenicia, F., Heitz, S., Plaza, D., de Keyser, R., Pauwels, V. R. N., Wagner,
912 W. and Savenije, H.: Can ASCAT-derived soil wetness indices reduce predictive
913 uncertainty in well-gauged areas? A comparison with in situ observed soil moisture in an
914 assimilation application, *Adv. Water Resour.*, 44, 49–65,
915 doi:10.1016/j.advwatres.2012.03.022, 2012.

916 McCabe, M. F., Wood, E. F. and Gao, H.: Initial soil moisture retrievals from AMSR-E:
917 Multiscale comparison using in situ data and rainfall patterns over Iowa, *Geophys. Res.*
918 *Lett.*, 32(6), 1–4, doi:10.1029/2004GL021222, 2005.

919 Pan, M. and Wood, E. F.: Data Assimilation for Estimating the Terrestrial Water Budget
920 Using a Constrained Ensemble Kalman Filter, *J. Hydrometeorol.*, 7(3), 534–547,
921 doi:10.1175/JHM495.1, 2006.

922 Pan, M., Li, H. and Wood, E.: Assessing the skill of satellite-based precipitation
923 estimates in hydrologic applications, *Water Resour. Res.*, 46(9), W09535,
924 doi:10.1029/2009WR008290, 2010.

925 Pan, M., Sahoo, A. K. and Wood, E. F.: Improving soil moisture retrievals from a
926 physically-based radiative transfer model, *Remote Sens. Environ.*, 140, 130–140,
927 doi:10.1016/j.rse.2013.08.020, 2014.

928 Pellarin, T., Ali, A., Chopin, F., Jobard, I. and Bergès, J. C.: Using spaceborne surface
 929 soil moisture to constrain satellite precipitation estimates over West Africa, *Geophys.*
 930 *Res. Lett.*, 35(2), 3–7, doi:10.1029/2007GL032243, 2008.

931 Pellarin, T., Louvet, S., Gruhier, C., Quantin, G. and Legout, C.: A simple and effective
 932 method for correcting soil moisture and precipitation estimates using AMSR-E
 933 measurements, *Remote Sens. Environ.*, 136, 28–36, doi:10.1016/j.rse.2013.04.011, 2013.

934 Robock, A., Luo, L., Wood, E. F., Wen, F., Mitchell, K., Houser, P., Schaake, J.,
 935 Lohmann, D., Cosgrove, B., Sheffield, J., Duan, Q., Higgins, W., Pinker, R., Tarpley, D.,
 936 Basara, J. and Crawford, K.: Evaluation of the North American Land Data Assimilation
 937 System over the southern Great Plains during the warm season, *J. Geophys. Res.*,
 938 108(D22), 8846, doi:10.1029/2002JD003245, 2003.

939 Schaake, J. C., Duan, Q., Koren, V., Mitchell, K. E., Houser, P. R., Wood, E. F., [Robock,](#)
 940 [A., Lettenmaier, D. P., Lohmann, D., Cosgrove, B., Sheffield, J., Luo, L., Higgins, R. W.,](#)
 941 [Pinker, R. T., and Tarpley, J. D.:](#) An intercomparison of soil moisture fields in the North
 942 [American Land Data Assimilation System \(NLDAS\),](#) *J. Geophys. Res. Atmos.*, 109(D1),
 943 doi:10.1029/2002JD003309, 2004.

944 [Schamm, K., M. Ziese, A. Becker, P. Finger, A. Meyer-Christoffer, U. Schneider, M.](#)
 945 [Schröder, and P. Stender \(2014\),](#) Global gridded precipitation over land: A description of
 946 [the new GPCP First Guess Daily product,](#) *Earth Syst. Sci. Data*, 6, 49–60

947 [Sorooshian, S.:](#) Commentary-GEWEX (Global Energy and Water Cycle Experiment) at
 948 the 2004 Joint Scientific Committee Meeting, *GEWEX Newsl.*, 14(2), 2, 2004.

949 Wanders, N., Pan, M. and Wood, E. F.: Correction of real-time satellite precipitation with
 950 multi-sensor satellite observations of land surface variables, *Remote Sens. Environ.*, 160,
 951 206–221, doi:10.1016/j.rse.2015.01.016, 2015.

952 Wu, H., Adler, R. F., Tian, Y., Huffman, G. J., Li, H. and Wang, J.: Real-time global
 953 flood estimation using satellite-based precipitation and a coupled land surface and routing
 954 model. *Water Resour. Res.*, 50(3), 2693-2717, doi:10.1002/2013WR014710, 2014.

955

Authors 8/31/2015 3:38 PM
 Deleted: . Y

Authors 8/31/2015 3:38 PM
 Moved (insertion) [2]

Authors 8/31/2015 3:38 PM
 Moved (insertion) [3]

Authors 8/31/2015 3:38 PM
 Moved (insertion) [4]

Authors 8/31/2015 3:38 PM
 Moved (insertion) [5]

Authors 8/31/2015 3:38 PM
 Moved up [2]: Robock, A., Lettenmaier, D. P., Lohmann, D., Cosgrove, B.,

Authors 8/31/2015 3:38 PM
 Moved up [3]: Higgins, R. W., Pinker, R. T

Authors 8/31/2015 3:38 PM
 Deleted: .,

Authors 8/31/2015 3:38 PM
 Moved up [4]: and Tarpley, J. D.: An intercomparison of soil moisture fields in the North American Land Data

Authors 8/31/2015 3:38 PM
 Moved up [5]: Geophys.

Authors 8/31/2015 3:38 PM
 Deleted: She eld, J., Luo, L. F.,

Authors 8/31/2015 3:38 PM
 Deleted: Assimilation System (NLDAS), J.

Authors 8/31/2015 3:38 PM
 Deleted: Res., 109(D1), D01S90, doi:10.1029/2002JD003309, 2004. .

Authors 8/31/2015 3:38 PM
 Deleted: —————Page Break—————

971 **List of Tables**

972 **Tables**

973 Table 1 Error statistics of recovered precipitation and effect of surface saturation in the idealized experiment (mm/day).

974 Table 2 Error statistics of recovered NLDAS based on ΔSM (with added errors) conditioned on 1st layer soil wetness for the idealized
975 experiment (mm/day).

976 Table 3 Error statistics of 3B42RT and 3B42RT_{ADJ} compared to NLDAS precipitation (mm/day)

Authors 8/31/2015 3:38 PM
Deleted:
Unknown
Formatted: Font:(Default) Helvetica, 6 pt

978 [List of Figures](#)

979 Figure 1 Schematic for [the](#) dynamic assimilation of AMSR-E/LSMEM Δ SM into TMPA
980 (3B42RT) [with the particle filter \(PF\)](#).

981 Figure 2 Schematic for [the strategy for processing](#) prior and posterior probability
982 [densities](#) in [the](#) particle filter.

983 Figure 3 Statistics of NLDAS precipitation given 3B42RT precipitation measurement.
984 Boxplot shows the minimum, 15% quantile, 30% quantile, median, 70% quantile, 85%
985 quantile and maximum value of NLDAS precipitation given 3B42RT precipitation in a
986 certain bin.

987 Figure 4 Empirical cumulative distribution function of changes in soil moisture from top
988 layer soil moisture from NLDAS precipitation forced VIC simulation (black), and
989 AMSR-E/LSMEM soil moisture retrieval before (red) and after (blue) pre-processing.

990 Figure 5 Two cases with recovered spatial rainfall pattern in [the](#) idealized experiment
991 after merging satellite soil moisture retrieval on: (a-e) 27th Oct. 2003 and (f-j) 22th Mar.
992 2006.

993 [Figure 6 Accuracy of recovered precipitation in idealized experiment: \(a\) overall](#)
994 [performance and separately comparing the improvement performance of recovered](#)
995 [NLDAS precipitation \(b\) with and \(c\) without surface saturation condition. Statistics](#)
996 [provided in Table 1.](#)

997 Figure 7 Error in recovered NLDAS precipitation given surface moisture condition.
998 Recovered NLDAS is based on using “truth” soil moisture and soil moisture with normal
999 error: $N(0, \text{1mm})$, $N(0, \text{2mm})$, $N(0, \text{3mm})$, $N(0, \text{4mm})$ and $N(0, \text{5mm})$. Statistics provided in
1000 Table 2.

1001 | Figure 8 May 26th 2006 Rainfall pattern in 3B42RT (b) against NLDAS (d) as detected
1002 | by AMSR-E/LSMEM Δ SM (a), and recovered rainfall field ($3B42RT_{ADJ}$) by assimilating
1003 | AMSR-E/LSMEM Δ SM (c). Gray shading shows area without soil moisture retrievals.
1004 | Figure 9 [Pearson correlation coefficient between AMSR-E/LSMEM \$\Delta\$ SM and](#)
1005 | [precipitation: a\) NLDAS, b\) 3B42RT and c\) 3B42RT_{ADJ}; annual mean precipitation in d\)](#)
1006 | [NLDAS, e\) 3B42RT and f\) 3B42RT_{ADJ} of time steps with AMSR-E/LSMEM \$\Delta\$ SM](#)
1007 | [retrievals.](#)
1008 | Figure 10 [Frequency of rainy days in 3B42RT, 3B42RT_{ADJ} and NLDAS with a\) 0.1](#)
1009 | [mm/day and b\) 2 mm/day rainfall threshold to define a rain day.](#)
1010 | Figure 11 Distribution of 3B42RT and 3B42RT_{ADJ} precipitation error compared to
1011 | NLDAS. Statistics are provided in Table 3.
1012 | Figure 12 [FAR and POD of 3B42RT and 3B42RT_{ADJ} with a\) 0.1 mm/day and b\) 2](#)
1013 | [mm/day rainfall threshold to define a rain event.](#)
1014 | Figure 13 [Probability that the added rainy days \(\$3B42RT = 0\$ mm/day, \$3B42RT_{ADJ} > 0\$](#)
1015 | [mm/day\) are true rain events \(\$NLDAS > 0\$ mm/day\) given corresponding AMSR-](#)
1016 | [E/LSMEM \$\Delta\$ SM.](#)
1017 |

Tables

Table 1 Error statistics of recovered precipitation and effect of surface saturation in the idealized experiment (mm/day).

		0	0~0.2	0.2~0.5	0.5~1.0	1.0~1.5	1.5~2	2~2.5	2.5~5.0	5.0~7.5	7.5~10	10~15	15~20	20~25	>25
[Recovered NLDAS]-[NLDAS]															
All surface conditions	Bias	0.24	0.20	0.37	0.51	0.71	0.87	1.09	0.67	1.16	1.30	2.51	3.32	3.75	3.95
	MAE	0.40	0.42	0.66	0.86	1.14	1.41	1.70	1.48	2.24	2.63	4.21	5.56	6.70	9.76
Unsaturated surface	Bias	0.23	0.19	0.29	0.40	0.52	0.68	0.82	0.65	1.10	1.27	2.19	2.88	3.14	3.14
	MAE	0.39	0.41	0.59	0.75	0.95	1.21	1.43	1.45	2.17	2.58	3.88	5.11	6.07	8.94
Saturated surface	Bias	2.31	5.06	47.65	42.58	50.67	44.09	59.64	6.83	16.09	9.19	46.47	57.98	65.33	64.09
	MAE	3.35	5.54	48.71	43.73	52.43	46.96	61.85	9.64	21.42	15.01	49.07	60.78	69.53	70.73

Deleted: <sp>

Unknown

Formatted ... [3]

Authors 8/31/2015 3:38 PM

Formatted Table ... [4]

Authors 8/31/2015 3:38 PM

Formatted ... [5]

Authors 8/31/2015 3:38 PM

Formatted ... [6]

Authors 8/31/2015 3:38 PM

Formatted ... [7]

Authors 8/31/2015 3:38 PM

Formatted ... [15]

Authors 8/31/2015 3:38 PM

Formatted ... [8]

Authors 8/31/2015 3:38 PM

Formatted ... [9]

Authors 8/31/2015 3:38 PM

Formatted ... [10]

Authors 8/31/2015 3:38 PM

Formatted ... [11]

Authors 8/31/2015 3:38 PM

Formatted ... [12]

Authors 8/31/2015 3:38 PM

Formatted ... [13]

Authors 8/31/2015 3:38 PM

Formatted ... [14]

Authors 8/31/2015 3:38 PM

Formatted ... [16]

Authors 8/31/2015 3:38 PM

Formatted ... [17]

Authors 8/31/2015 3:38 PM

Formatted ... [18]

Authors 8/31/2015 3:38 PM

Formatted ... [19]

Authors 8/31/2015 3:38 PM

Deleted: 092

Authors 8/31/2015 3:38 PM

Deleted: 155

Authors 8/31/2015 3:38 PM

Formatted ... [20]

Authors 8/31/2015 3:38 PM

Deleted: 238

Authors 8/31/2015 3:38 PM

Formatted ... [21]

Authors 8/31/2015 3:38 PM

Formatted ... [22]

Authors 8/31/2015 3:38 PM

Authors 8/31/2015 3:38 PM

Formatted ... [23]

Authors 8/31/2015 3:38 PM

Formatted

Table 2 Error statistics of recovered NLDAS based on ΔSM (with added errors) conditioned on 1st layer soil wetness for the idealized experiment (mm/day).

		[VIC 1st layer SM] <-30	-30~-25	-25~-20	-20~-15	-15~-12	-12~-10	-10~-9	-9~-8	>-8
	[Recovered NLDAS]-[NLDAS] [mm/day]									
No error	Median	0.04	0.03	0.02	0.02	0.02	0.03	0.03	0.04	0.16
	IQR	0.14	0.08	0.07	0.07	0.08	0.12	0.21	0.29	1.71
1.0	Median	0.86	1.07	1.08	1.03	0.99	0.97	0.97	0.94	0.66
	IQR	1.52	1.72	1.77	1.83	1.96	2.08	2.14	2.19	2.59
2.0	Median	0.68	1.07	1.40	1.56	1.52	1.44	1.51	1.64	1.54
	IQR	1.76	2.09	2.88	3.45	3.63	3.73	3.73	3.73	3.91
3.0	Median	0.15	0.80	1.20	1.41	1.47	1.51	1.65	1.84	1.88
	IQR	1.36	2.16	3.04	3.73	3.74	3.79	4.34	5.24	5.47
4.0	Median	0.22	0.56	0.83	1.15	1.30	1.40	1.63	1.88	1.97
	IQR	0.99	2.36	2.48	3.99	4.05	4.70	5.53	5.52	5.63
5.0	Median	0.00	0.15	0.52	0.90	1.10	1.27	1.54	1.81	1.89
	IQR	1.62	2.54	2.91	4.43	4.51	5.95	5.90	5.79	7.04

*1st layer soil depth is 100mm with a SM capacity of ~45mm depending on porosity.

Formatted ... [113]

Authors 8/31/2015 3:38 PM

Deleted: <sp> - ... [114]

Unknown

Formatted ... [115]

Authors 8/31/2015 3:38 PM

Formatted Table ... [116]

Unknown

Formatted ... [117]

Authors 8/31/2015 3:38 PM

Formatted ... [118]

Authors 8/31/2015 3:38 PM

Formatted ... [119]

Authors 8/31/2015 3:38 PM

Formatted ... [120]

Authors 8/31/2015 3:38 PM

Formatted ... [121]

Authors 8/31/2015 3:38 PM

Formatted ... [122]

Authors 8/31/2015 3:38 PM

Formatted ... [123]

Authors 8/31/2015 3:38 PM

Formatted ... [124]

Authors 8/31/2015 3:38 PM

Formatted ... [125]

Authors 8/31/2015 3:38 PM

Formatted ... [126]

Deleted: 035

Authors 8/31/2015 3:38 PM

Deleted: 041

Authors 8/31/2015 3:38 PM

Formatted ... [137]

Authors 8/31/2015 3:38 PM

Deleted: 159

Authors 8/31/2015 3:38 PM

Formatted ... [130]

Authors 8/31/2015 3:38 PM

Deleted: 027

Authors 8/31/2015 3:38 PM

Deleted: 023

Authors 8/31/2015 3:38 PM

Formatted ... [131]

Authors 8/31/2015 3:38 PM

Deleted: 019

Authors 8/31/2015 3:38 PM

Formatted ... [133]

Authors 8/31/2015 3:38 PM

Authors 8/31/2015 3:38 PM

Formatted ... [127]

Authors 8/31/2015 3:38 PM

Formatted

Table 3 Error statistics of 3B42RT and 3B42RT_{ADJ} compared to NLDAS precipitation (mm/day)

[3B42RT] - [NLDAS] [mm/day]	<-25	-25~-	-20~-	-15~-	-10~-	-5~-2	-2~-	-	0.5~2	2~5	5~10	10~1	15~2	20~2	>25
	20	15	10	5	0.5	0.5~0	.5					5	0	5	
[3B42RT] - Mean	-32.32	-22.19	-17.13	-12.09	-6.98	-3.22	-1.09	-0.02	1.11	3.20	6.87	11.96	16.97	21.95	27.35
[NLDAS] STD	8.52	1.42	1.42	1.42	1.39	0.85	0.43	0.12	0.43	0.84	1.37	1.39	1.37	1.38	2.08
[3B42RT _{ADJ}] - Mean	-31.24	-20.31	-14.79	-9.69	-4.81	-1.60	0.16	1.08	0.44	0.21	0.02	-0.06	0.00	-0.03	-0.12
[NLDAS] STD	11.03	6.40	6.12	5.34	4.08	2.73	1.88	1.18	1.86	2.29	2.60	2.91	3.01	2.74	2.41

Formatted ... [245]

Authors 8/31/2015 3:38 PM

Formatted ... [249]

Authors 8/31/2015 3:38 PM

Formatted ... [251]

Authors 8/31/2015 3:38 PM

Formatted ... [252]

Authors 8/31/2015 3:38 PM

Formatted ... [253]

Authors 8/31/2015 3:38 PM

Formatted ... [255]

Authors 8/31/2015 3:38 PM

Formatted ... [260]

Authors 8/31/2015 3:38 PM

Formatted ... [256]

Authors 8/31/2015 3:38 PM

Formatted ... [258]

Authors 8/31/2015 3:38 PM

Formatted ... [259]

Authors 8/31/2015 3:38 PM

Formatted ... [262]

Authors 8/31/2015 3:38 PM

Formatted ... [263]

Authors 8/31/2015 3:38 PM

Formatted ... [246]

Authors 8/31/2015 3:38 PM

Formatted ... [250]

Authors 8/31/2015 3:38 PM

Formatted Table ... [247]

Authors 8/31/2015 3:38 PM

Formatted ... [261]

Authors 8/31/2015 3:38 PM

Formatted ... [264]

Authors 8/31/2015 3:38 PM

Formatted ... [265]

Authors 8/31/2015 3:38 PM

Formatted ... [266]

Authors 8/31/2015 3:38 PM

Formatted ... [267]

Authors 8/31/2015 3:38 PM

Formatted ... [268]

Authors 8/31/2015 3:38 PM

Formatted ... [269]

Authors 8/31/2015 3:38 PM

Formatted ... [248]

Authors 8/31/2015 3:38 PM

Formatted ... [254]

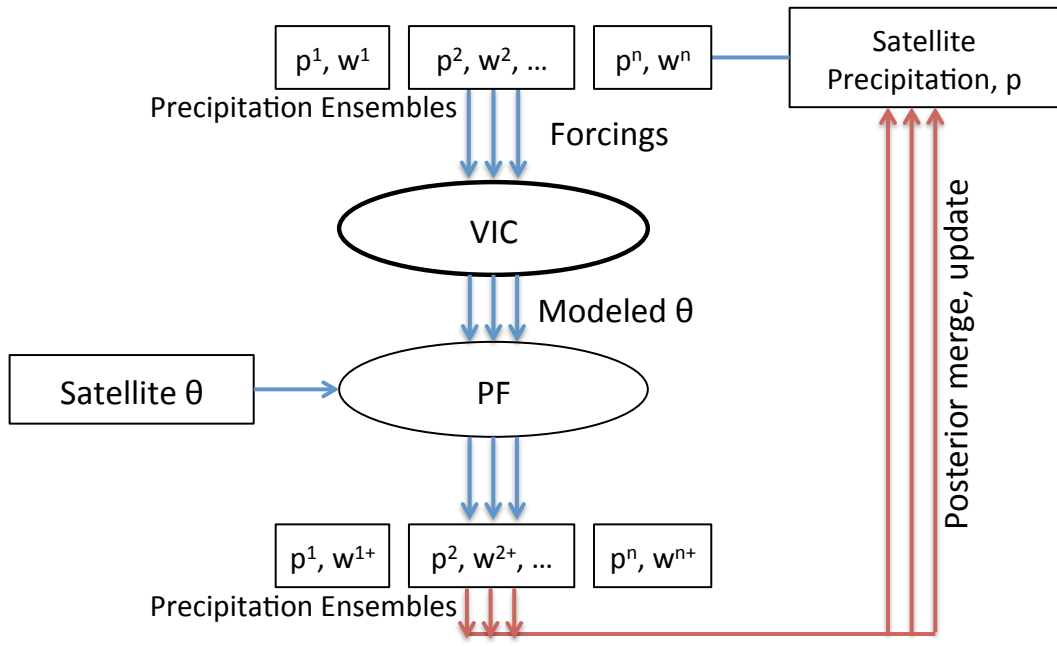
Authors 8/31/2015 3:38 PM

Formatted ... [257]

Authors 8/31/2015 3:38 PM

Formatted ... [274]

Authors 8/31/2015 3:38 PM



1545

1546 Figure 1 Schematic for the dynamic assimilation of AMSR-E/LSMEM Δ SM into TMPA (3B42RT) with the particle filter (PF).

1547

Authors 8/31/2015 3:38 PM

p^1, w^1
Precipitation Er

Satellite θ

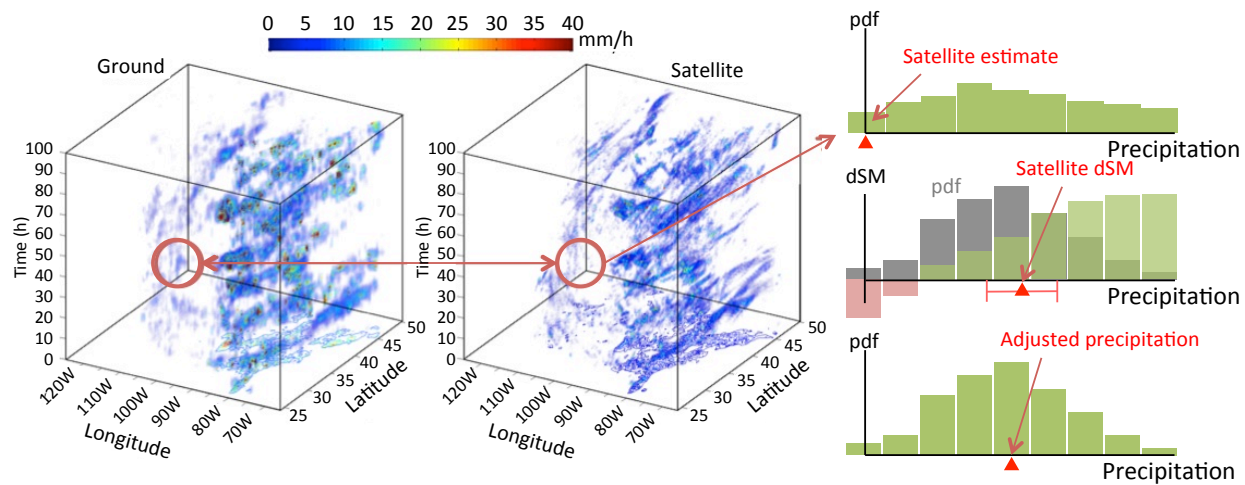
p^1, w^1
Precipitation Er

Deleted:

Authors 8/31/2015 3:38 PM
Deleted: of particle filtering

Authors 8/31/2015 3:38 PM
Deleted: Page Break

... [337]

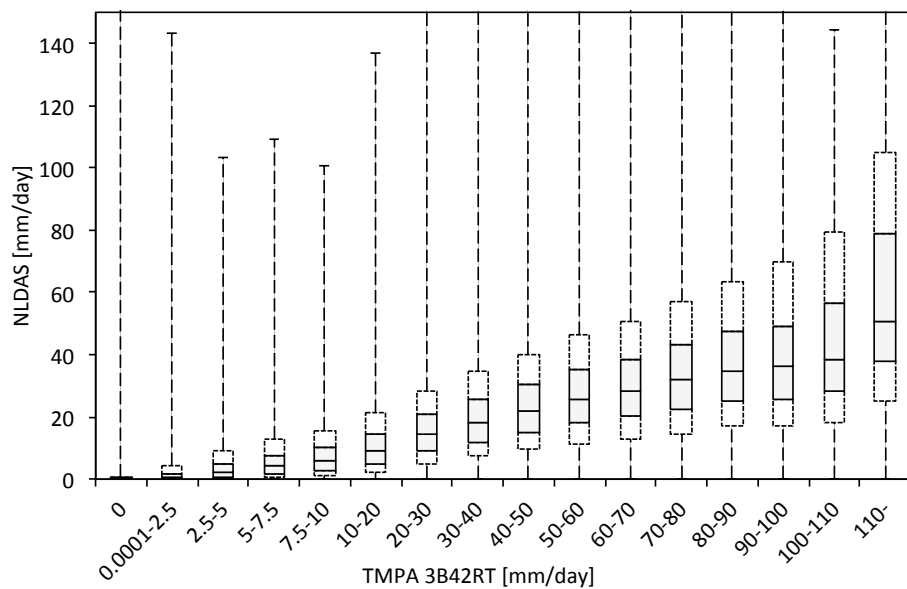


1553

1554 Figure 2 Schematic for [the strategy for processing](#) prior and posterior probability [densities](#) in [the](#) particle filter.

1555

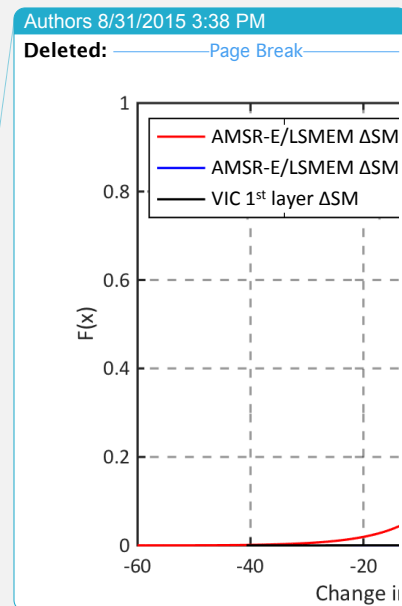
Authors 8/31/2015 3:38 PM
Deleted: handling
 Authors 8/31/2015 3:38 PM
Deleted: density handling strategy
 Authors 8/31/2015 3:38 PM
Deleted: Page Break
 ... [338]

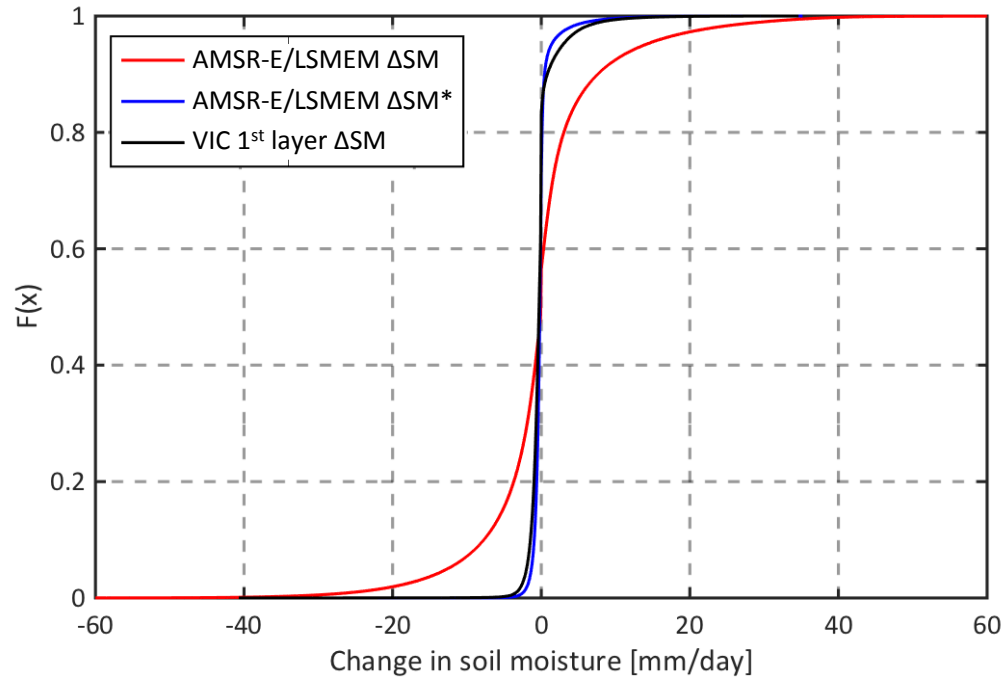


1561

1562 Figure 3 Statistics of NLDAS precipitation given 3B42RT precipitation measurement. Boxplot shows the minimum, 15% quantile,
 1563 30% quantile, median, 70% quantile, 85% quantile and maximum value of NLDAS precipitation given 3B42RT precipitation in a
 1564 certain bin.

1565

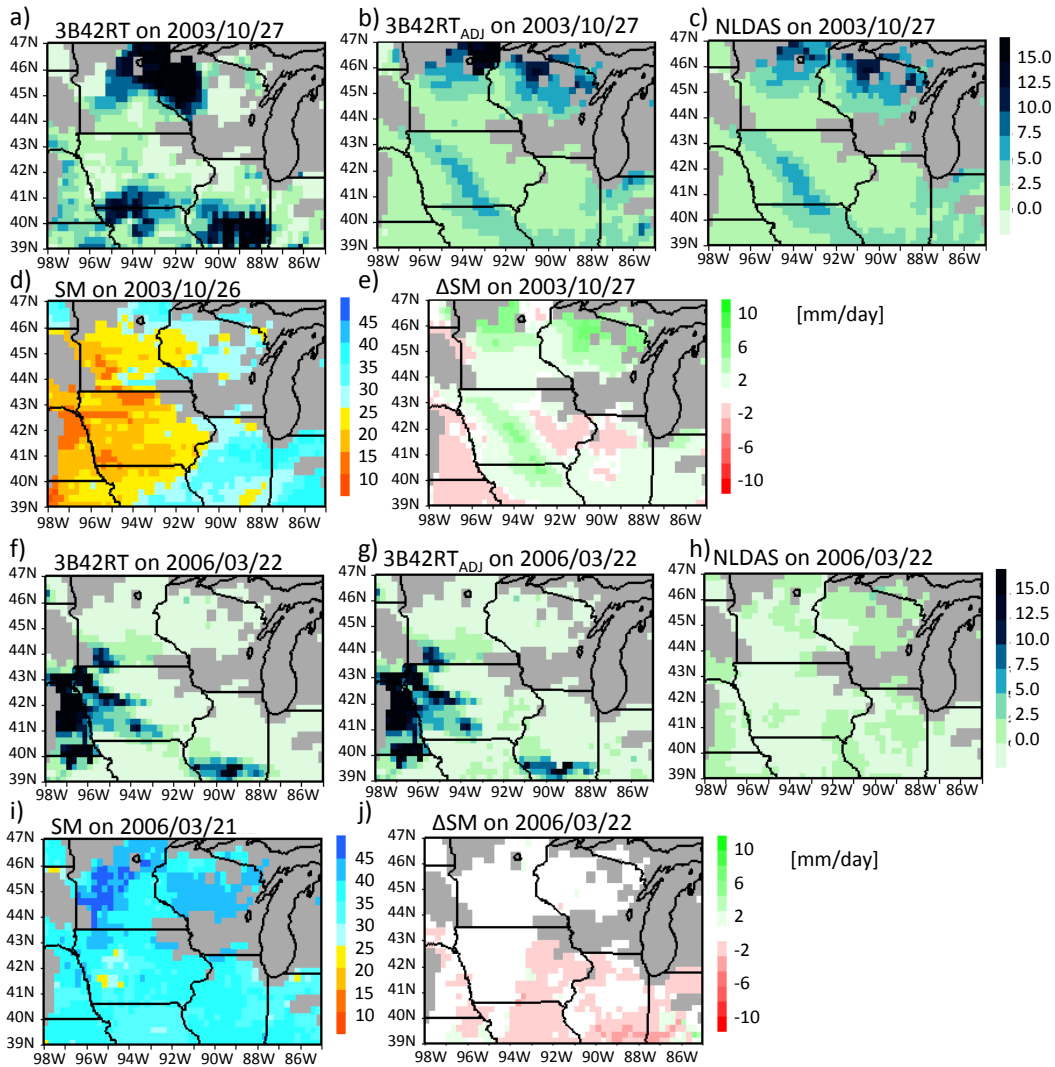




1568

1569 Figure 4 Empirical cumulative distribution function of changes in soil moisture from top layer soil moisture from NLDAS
 1570 precipitation forced VIC simulation (black), and AMSR-E/LSMEM soil moisture retrieval before (red) and after (blue) pre-
 1571 processing.

1572



576

577 Figure 5 Two cases with recovered spatial rainfall pattern in [the](#) idealized experiment after merging satellite
 578 soil moisture retrieval on: (a-e) 27th Oct. 2003 and (f-j) 22th Mar. 2006.

579

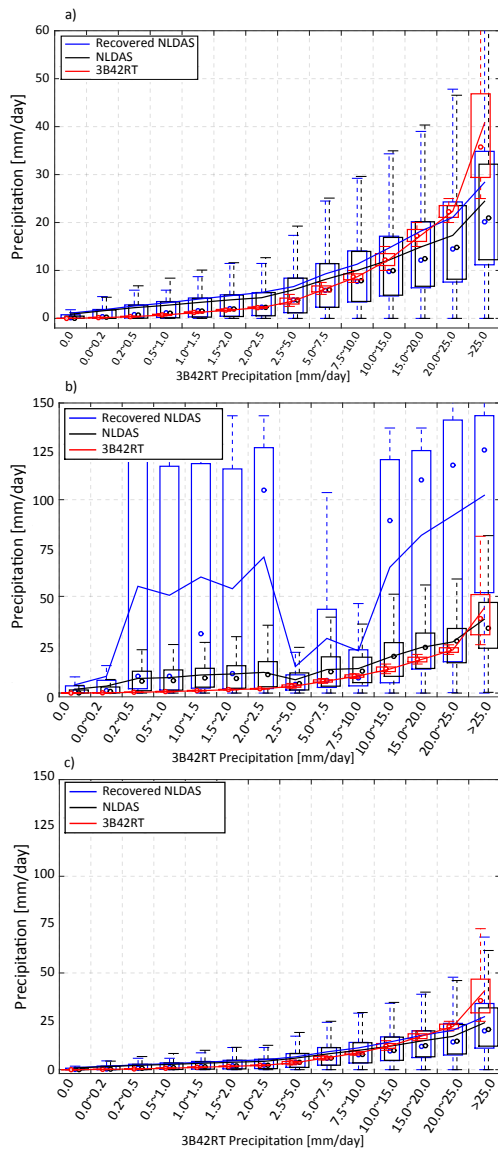
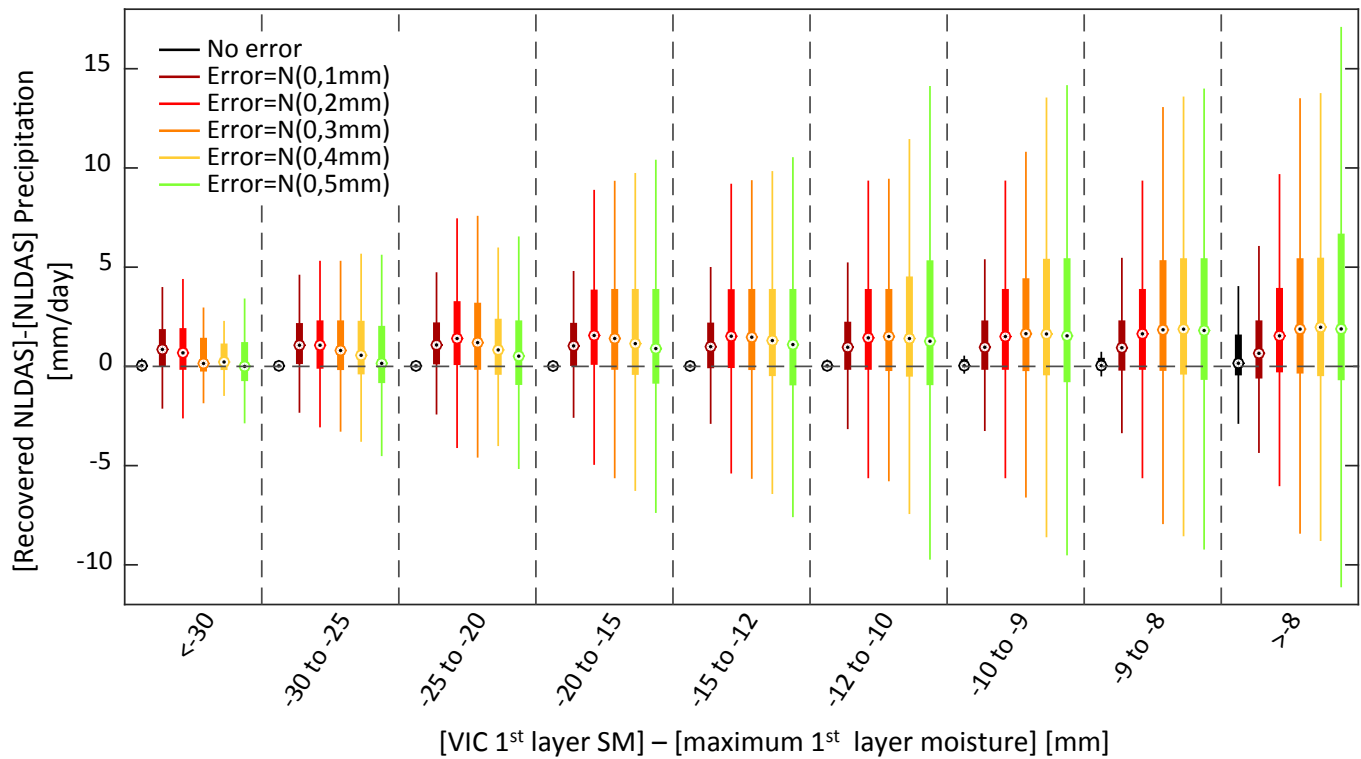


Figure 6 Accuracy of recovered precipitation in idealized experiment: (a) overall performance and separately comparing the improvement performance of recovered NLDAS precipitation (b) with and (c) without surface saturation condition. Statistics provided in Table 1.

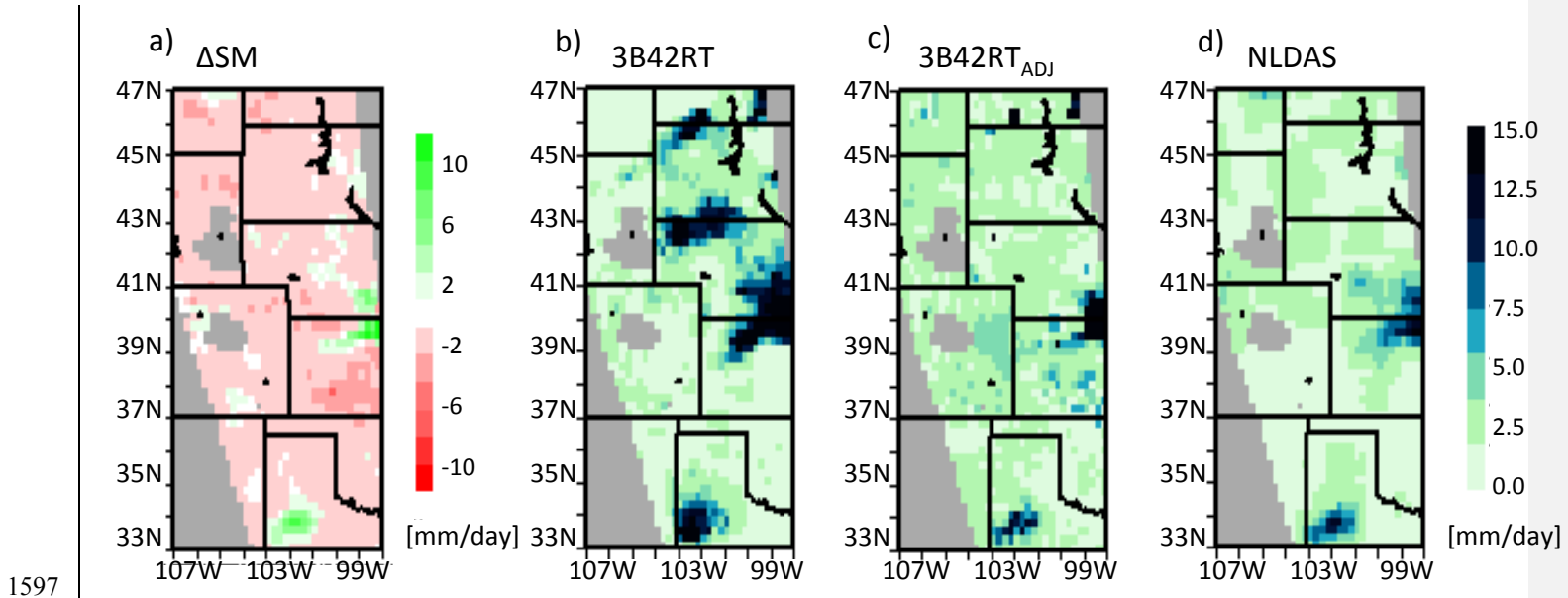


1584

1585 Figure 7 Error in recovered NLDAS precipitation given surface moisture condition. Recovered NLDAS is based on using “truth” soil
 1586 moisture and soil moisture with normal error: $N(0,1mm)$, $N(0,2mm)$, $N(0,3mm)$, $N(0,4mm)$ and $N(0,5mm)$. Statistics provided in
 1587 Table 2.

1588

Authors 8/31/2015 3:38 PM
Formatted: Left
 Authors 8/31/2015 3:38 PM
Deleted: .5mm
 Authors 8/31/2015 3:38 PM
Deleted: 1.0mm
 Authors 8/31/2015 3:38 PM
Deleted: 1.5mm), $N(0,2.0mm)$, $N(0,2.5mm)$,
 $N(0,3.0mm)$, $N(0,3.5mm)$, $N(0,4.0mm)$,
 $N(0,4.5mm)$
 Authors 8/31/2015 3:38 PM
Deleted: 5.0mm
 Authors 8/31/2015 3:38 PM
Deleted: Page Break

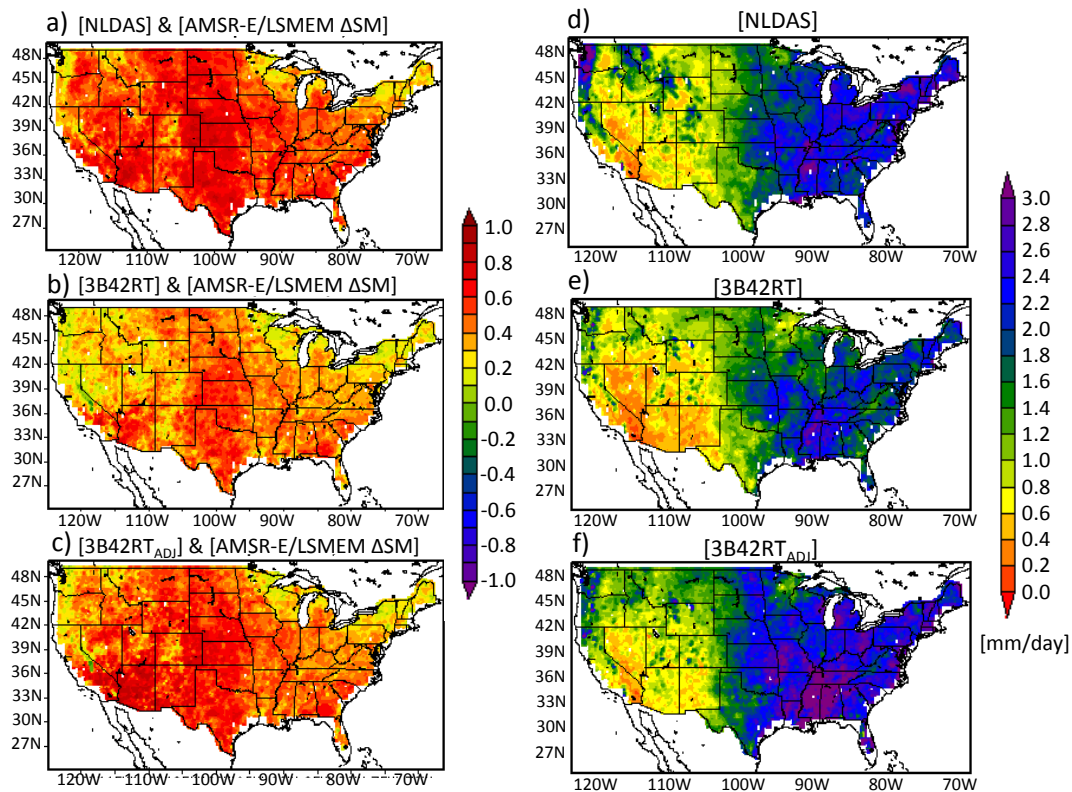


1597

1598 Figure 8 May 26th 2006 Rainfall pattern in 3B42RT (b) against NLDAS (d) as detected by AMSR-E/LSMEM Δ SM (a), and recovered
 1599 rainfall field (3B42RT_{ADJ}) by assimilating AMSR-E/LSMEM Δ SM (c). Gray shading shows area without soil moisture retrievals.

1600

Authors 8/31/2015 3:38 PM
 Deleted: into TMPA
 Authors 8/31/2015 3:38 PM
 Deleted: Page Break
 ... [341]



1605

1606

1607

1608

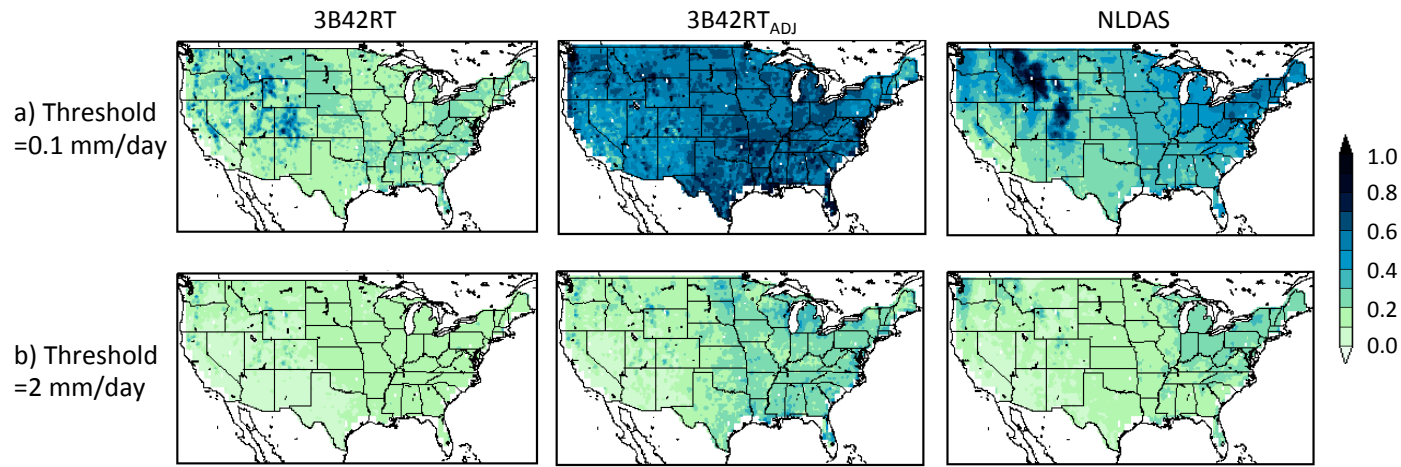
Figure 9 Pearson correlation coefficient between AMSR-E/LSMEM Δ SM and precipitation: a) NLDAS, b) 3B42RT and c) 3B42RT_{ADJ}; annual mean precipitation in d) NLDAS, e) 3B42RT and f) 3B42RT_{ADJ} of time steps with AMSR-E/LSMEM Δ SM retrievals.

Authors 8/31/2015 3:38 PM

Deleted: FAR, POD

Authors 8/31/2015 3:38 PM

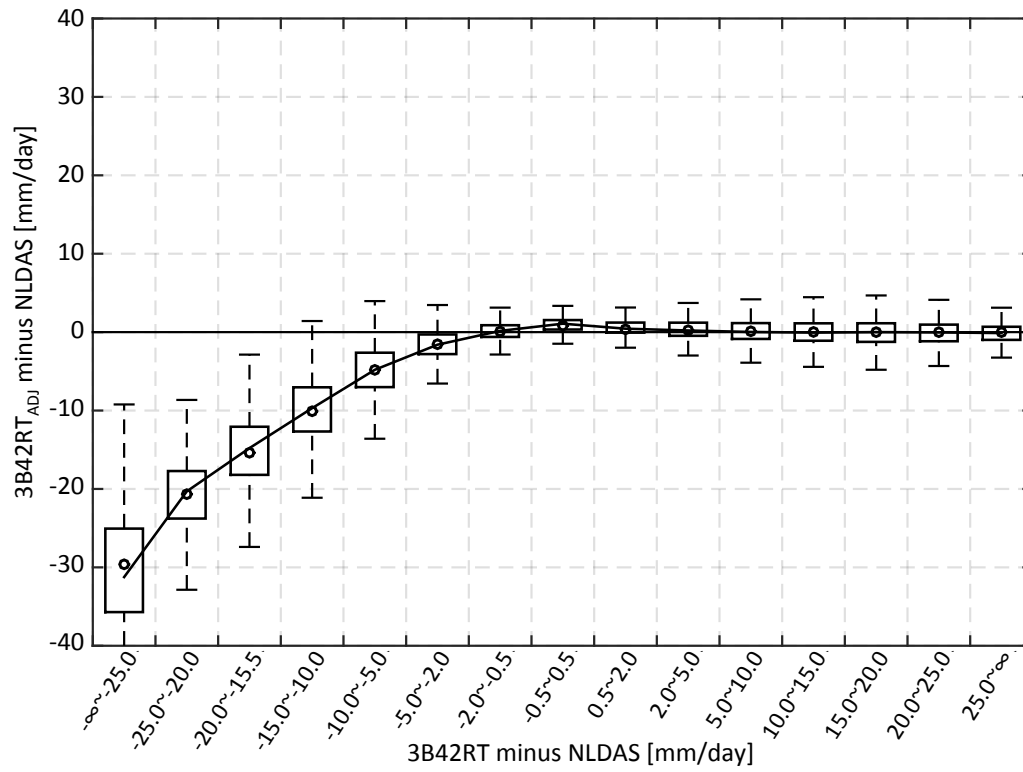
Deleted: frequency of rainy days



1611
1612
1613
1614

Figure 10 Frequency of rainy days in 3B42RT, 3B42RT_{ADJ} and NLDAS with a) 0.1 mm/day and b) 2 mm/day rainfall threshold to define a rain day.

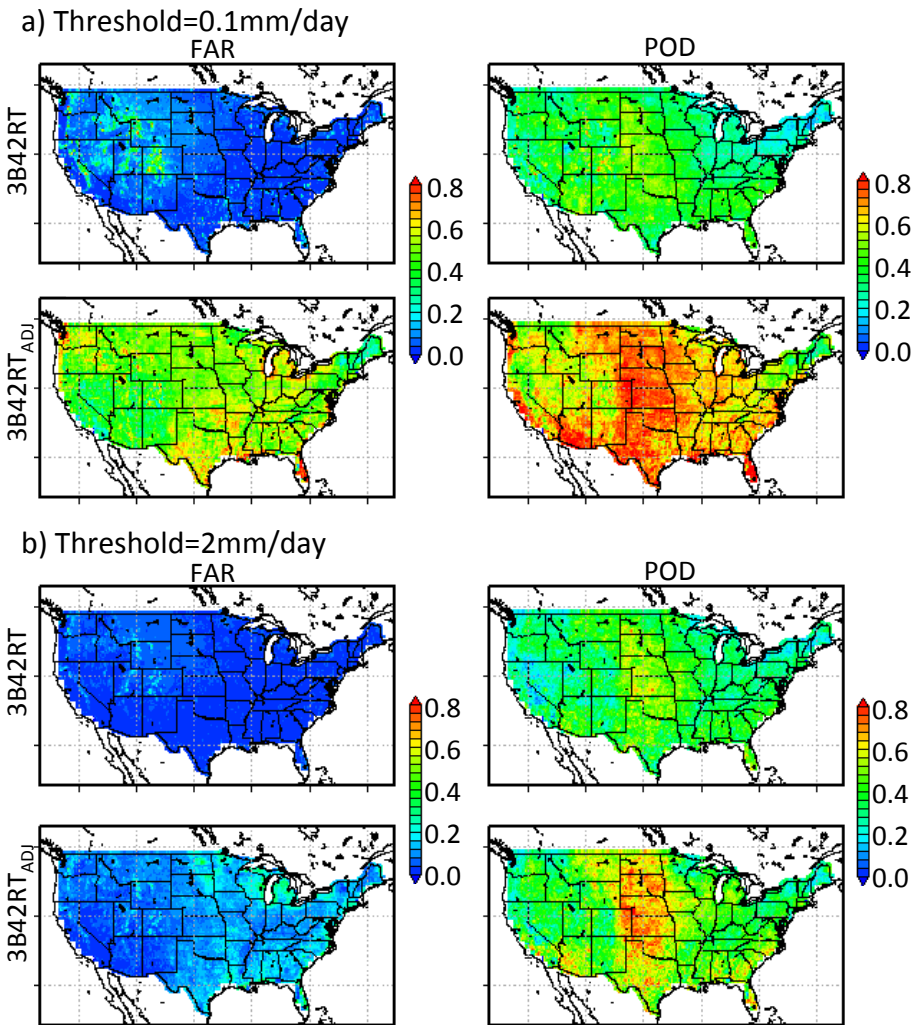
- Authors 8/31/2015 3:38 PM
- Deleted:** 1mm
- Authors 8/31/2015 3:38 PM
- Deleted:** (top)
- Authors 8/31/2015 3:38 PM
- Deleted:** 2mm
- Authors 8/31/2015 3:38 PM
- Deleted:** (bottom)
- Authors 8/31/2015 3:38 PM
- Deleted:** event
- Authors 8/31/2015 3:38 PM
- Deleted:** [342]



1622

1623 Figure 11 Distribution of 3B42RT and 3B42RT_{ADJ} precipitation error compared to NLDAS. Statistics are provided in Table 3.

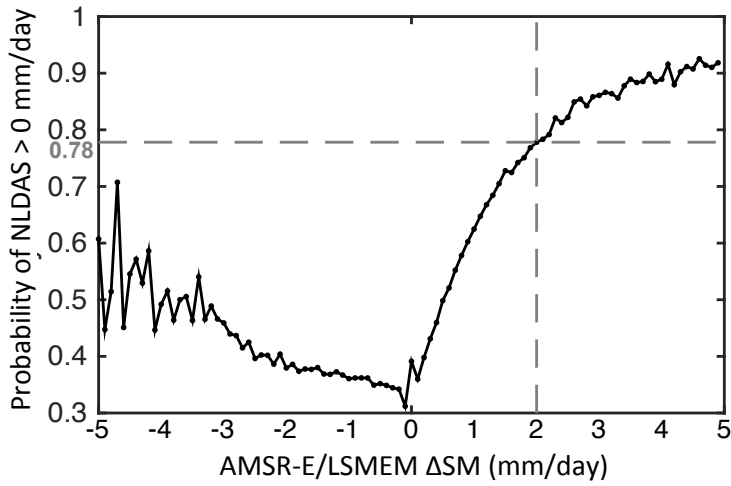
1624



1628
1629
1630

Figure 12 FAR and POD of 3B42RT and 3B42RT_{ADJ} with a) 0.1 mm/day and b) 2 mm/day rainfall threshold to define a rain event.

- Authors 8/31/2015 3:38 PM
Deleted: (a-b) Difference in mean absolute error
- Authors 8/31/2015 3:38 PM
Deleted: and 3B42RT compared to NLDAS (MAE(3B42RT_{ADJ})-MAE(3B42RT)); (c-d) same as (a-b), after 2mm
- Authors 8/31/2015 3:38 PM
Deleted: cutoff ΔSM
- Authors 8/31/2015 3:38 PM
Deleted: is applied



1638

1639

1640

1641

Figure 13 Probability that the added rainy days ($3B42RT = 0$ mm/day, $3B42RT_{ADJ} > 0$ mm/day) are true rain events ($NLDAS > 0$ mm/day) given corresponding AMSR-E/LSMEM Δ SM.

Authors 8/31/2015 3:38 PM
 Deleted: Page Break
 ... [344]

Authors 8/31/2015 3:38 PM
 Deleted: Distribution of

Authors 8/31/2015 3:38 PM
 Deleted: when rainy days are added in $3B42RT_{ADJ}$ (no rain in $3B42RT$, rain in $3B42RT_{ADJ}$)

Authors 8/31/2015 3:38 PM
 Deleted: ... [345]